Yield Strength Engineering

Cierra Cowell

First Edition, 2012

ISBN 978-81-323-4414-8

Published by:
White Word Publications
4735/22 Prakashdeep Bldg,
Ansari Road, Darya Ganj,
Delhi - 110002
Email: info@wtbooks.com

Table of Contents

Chapter 1

Hill Yield Criteria

Rodney Hill has developed several yield criteria for anisotropic plastic deformations. The earliest version was a straightforward extension of the von Mises yield criterion and had a quadratic form. This model was later generalized by allowing for an exponent *m*. Variations of these criteria are in wide use for metals, polymers, and certain composites.

Quadratic Hill yield criterion

The quadratic Hill yield criterion. has the form

$$F(\sigma_{22}-\sigma_{33})^2+G(\sigma_{33}-\sigma_{11})^2+H(\sigma_{11}-\sigma_{22})^2+2L\sigma_{23}^2+2M\sigma_{31}^2+2N\sigma_{12}^2=1\ .$$

Here *F, G, H, L, M, N* are constants that have to be determined experimentally and σ_{ij} are the stresses. The quadratic Hill yield criterion depends only on the deviatoric stresses and is pressure independent. It predicts the same yield stress in tension and in compression.

Expressions for F, G, H, L, M, N

If the axes of material anisotropy are assumed to be orthogonal, we can write

$$(G+H)\ (\sigma_1^y)^2=1\ ;\quad (F+H)\ (\sigma_2^y)^2=1\ ;\quad (F+G)\ (\sigma_3^y)^2=1$$

where $\sigma_1^y, \sigma_2^y, \sigma_3^y$ are the normal yield stresses with respect to the axes of anisotropy. Therefore we have

$$F=\frac{1}{2}\left[\frac{1}{(\sigma_2^y)^2}+\frac{1}{(\sigma_3^y)^2}-\frac{1}{(\sigma_1^y)^2}\right]$$
$$G=\frac{1}{2}\left[\frac{1}{(\sigma_3^y)^2}+\frac{1}{(\sigma_1^y)^2}-\frac{1}{(\sigma_2^y)^2}\right]$$

$$H = \frac{1}{2}\left[\frac{1}{(\sigma_1^y)^2} + \frac{1}{(\sigma_2^y)^2} - \frac{1}{(\sigma_3^y)^2}\right]$$

Similarly, if $\tau_{12}^y, \tau_{23}^y, \tau_{31}^y$ are the yield stresses in shear (with respect to the axes of anisotropy), we have

$$L = \frac{1}{2\ (\tau_{23}^y)^2}\ ; \quad M = \frac{1}{2\ (\tau_{31}^y)^2}\ ; \quad N = \frac{1}{2\ (\tau_{12}^y)^2}$$

Quadratic Hill yield criterion for plane stress

The quadratic Hill yield criterion for thin rolled plates (plane stress conditions) can be expressed as

$$\sigma_1^2 + \frac{R_0\ (1 + R_{90})}{R_{90}\ (1 + R_0)}\ \sigma_2^2 - \frac{2\ R_0}{1 + R_0}\ \sigma_1\sigma_2 = (\sigma_1^y)^2$$

where the principal stresses σ_1,σ_2 are assumed to be aligned with the axes of anisotropy with σ_1 in the rolling direction and σ_2 perpendicular to the rolling direction, $\sigma_3 = 0$, R_0 is the R-value in the rolling direction, and R_{90} is the R-value perpendicular to the rolling direction.

For the special case of transverse isotropy we have $R = R_0 = R_{90}$ and we get

$$\sigma_1^2 + \sigma_2^2 - \frac{2\ R}{1 + R}\ \sigma_1\sigma_2 = (\sigma_1^y)^2$$

Generalized Hill yield criterion

The generalized Hill yield criterion has the form

$$\begin{aligned} F|\sigma_2 - \sigma_3|^m + G|\sigma_3 - \sigma_1|^m + H|\sigma_1 - \sigma_2|^m + L|2\sigma_1 - \sigma_2 - \sigma_3|^m \\ + M|2\sigma_2 - \sigma_3 - \sigma_1|^m + N|2\sigma_3 - \sigma_1 - \sigma_2|^m = \sigma_y^m\ . \end{aligned}$$

where σ_i are the principal stresses (which are aligned with the directions of anisotropy), σ_y is the yield stress, and *F, G, H, L, M, N* are constants. The value of *m* is determined by the degree of anisotropy of the material and must be greater than 1 to ensure convexity of the yield surface.

Generalized Hill yield criterion for plane stress

For transversely isotropic materials with 1 − 2 being the plane of symmetry, the generalized Hill yield criterion reduces to (with $F = G$ and $L = M$)

$$f := F|\sigma_2 - \sigma_3|^m + F|\sigma_3 - \sigma_1|^m + H|\sigma_1 - \sigma_2|^m + L|2\sigma_1 - \sigma_2 - \sigma_3|^m + L|2\sigma_2 - \sigma_3 - \sigma_1|^m + N|2\sigma_3 - \sigma_1 - \sigma_2|^m - \sigma_y^m \leq 0$$

The R-value or Lankford coefficient can be determined by considering the situation where $\sigma_1 > (\sigma_2 = \sigma_3 = 0)$. The R-value is then given by

$$R = \frac{(2^{m-1} + 2)L - N + H}{(2^{m-1} - 1)L + 2N + F}.$$

Under plane stress conditions and with some assumptions, the generalized Hill criterion can take several forms.

- **Case 1:** $L = 0, H = 0$.

$$f := \frac{1 + 2R}{1 + R}(|\sigma_1|^m + |\sigma_2|^m) - \frac{R}{1 + R}|\sigma_1 + \sigma_2|^m - \sigma_y^m \leq 0$$

- **Case 2:** $N = 0, F = 0$.

$$f := \frac{2^{m-1}(1 - R) + (R + 2)}{(1 - 2^{m-1})(1 + R)}|\sigma_1 - \sigma_2|^m - \frac{1}{(1 - 2^{m-1})(1 + R)}(|2\sigma_1 - \sigma_2|^m + |2\sigma_2 - \sigma_1|^m) - \sigma_y^m \leq 0$$

- **Case 3:** $N = 0, H = 0$.

$$f := \frac{2^{m-1}(1 - R) + (R + 2)}{(2 + 2^{m-1})(1 + R)}(|\sigma_1|^m - |\sigma_2|^m) + \frac{R}{(2 + 2^{m-1})(1 + R)}(|2\sigma_1 - \sigma_2|^m + |2\sigma_2 - \sigma_1|^m) - \sigma_y^m \leq 0$$

- **Case 4:** $L = 0, F = 0$.

$$f := \frac{1 + 2R}{2(1 + R)}|\sigma_1 - \sigma_2|^m + \frac{1}{2(1 + R)}|\sigma_1 + \sigma_2|^m - \sigma_y^m \leq 0$$

- **Case 5:** $L = 0, N = 0$.. This is the Hosford yield criterion.

$$f := \frac{1}{1 + R}(|\sigma_1|^m + |\sigma_2|^m) + \frac{R}{1 + R}|\sigma_1 - \sigma_2|^m - \sigma_y^m \leq 0$$

Care must be exercised in using these forms of the generalized Hill yield criterion because the yield surfaces become concave (sometimes even unbounded) for certain combinations of R and *m*.

Hill 1993 yield criterion

In 1993, Hill proposed another yield criterion for plane stress problems with planar anisotropy. The Hill93 criterion has the form

$$\left(\frac{\sigma_1}{\sigma_0}\right)^2 + \left(\frac{\sigma_2}{\sigma_{90}}\right)^2 + \left[(p+q-c) - \frac{p\sigma_1 + q\sigma_2}{\sigma_b}\right]\left(\frac{\sigma_1\sigma_2}{\sigma_0\sigma_{90}}\right) = 1$$

where σ_0 is the uniaxial tensile yield stress in the rolling direction, σ_{90} is the uniaxial tensile yield stress in the direction normal to the rolling direction, σ_b is the yield stress under uniform biaxial tension, and c,p,q are parameters defined as

$$c = \frac{\sigma_0}{\sigma_{90}} + \frac{\sigma_{90}}{\sigma_0} - \frac{\sigma_0\sigma_{90}}{\sigma_b^2}$$

$$\left(\frac{1}{\sigma_0} + \frac{1}{\sigma_{90}} - \frac{1}{\sigma_b}\right) \quad p = \frac{2R_0(\sigma_b - \sigma_{90})}{(1+R_0)\sigma_0^2} - \frac{2R_{90}\sigma_b}{(1+R_{90})\sigma_{90}^2} + \frac{c}{\sigma_0}$$

$$\left(\frac{1}{\sigma_0} + \frac{1}{\sigma_{90}} - \frac{1}{\sigma_b}\right) \quad q = \frac{2R_{90}(\sigma_b - \sigma_0)}{(1+R_{90})\sigma_{90}^2} - \frac{2R_0\sigma_b}{(1+R_0)\sigma_0^2} + \frac{c}{\sigma_{90}}$$

and R_0 is the R-value for uniaxial tension in the rolling direction, and R_{90} is the R-value for uniaxial tension in the in-plane direction perpendicular to the rolling direction.

Extensions of Hill's yield criteria

The original versions of Hill's yield criteria were designed for material that did not have pressure-dependent yield surfaces which are needed to model polymers and foams.

The Caddell-Raghava-Atkins yield criterion

An extension that allows for pressure dependence is Caddell-Raghava-Atkins (CRA) model which has the form

$$F(\sigma_{22}-\sigma_{33})^2+G(\sigma_{33}-\sigma_{11})^2+H(\sigma_{11}-\sigma_{22})^2+2L\sigma_{23}^2+2M\sigma_{31}^2+2N\sigma_{12}^2+I\sigma_{11}+J\sigma_{22}+K\sigma_{33}=1\,.$$

The Deshpande-Fleck-Ashby yield criterion

Another pressure-dependent extension of Hill's quadratic yield criterion which has a form similar to the Bresler Pister yield criterion is the Deshpande, Fleck and Ashby (DFA) yield criterion for honeycomb structures (used in sandwich composite construction). This yield criterion has the form

$$F(\sigma_{22}-\sigma_{33})^2+G(\sigma_{33}-\sigma_{11})^2+H(\sigma_{11}-\sigma_{22})^2+2L\sigma_{23}^2+2M\sigma_{31}^2+2N\sigma_{12}^2+K(\sigma_{11}+\sigma_{22}+\sigma_{33})^2=1\,.$$

Chapter 2

Hosford Yield Criterion

The Hosford yield criterion is a function that is used to determine whether a material has undergone plastic yielding under the action of stress.

Hosford yield criterion for isotropic plasticity

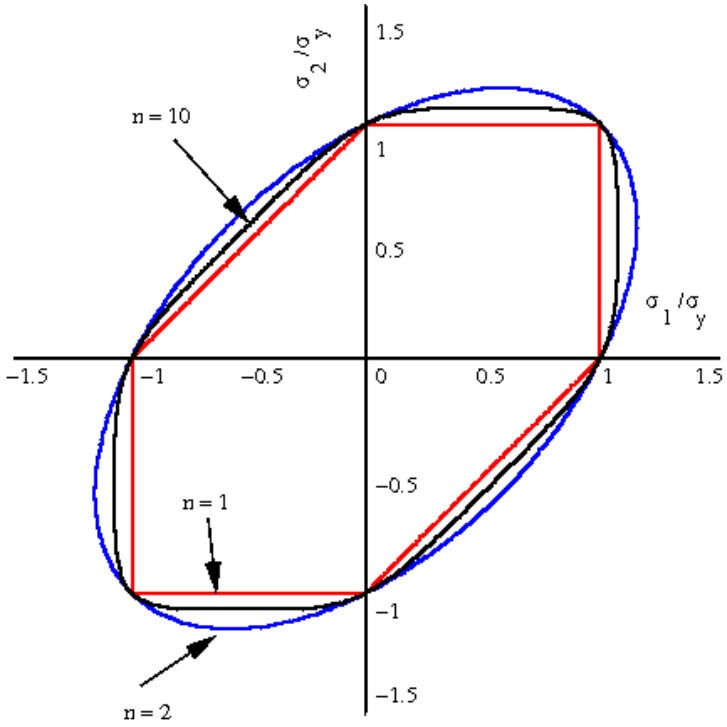

The plane stress, isotropic, Hosford yield surface for three values of *n*

The Hosford yield criterion for isotropic materials is a generalization of the von Mises yield criterion. It has the form

$$\tfrac{1}{2}|\sigma_2 - \sigma_3|^n + \tfrac{1}{2}|\sigma_3 - \sigma_1|^n + \tfrac{1}{2}|\sigma_1 - \sigma_2|^n = \sigma_y^n$$

where σ_i, i=1,2,3 are the principal stresses, *n* is a material-dependent exponent and σ_y is the yield stress in uniaxial tension/compression.

Alternatively, the yield criterion may be written as

$$\sigma_y = \left(\tfrac{1}{2}|\sigma_2 - \sigma_3|^n + \tfrac{1}{2}|\sigma_3 - \sigma_1|^n + \tfrac{1}{2}|\sigma_1 - \sigma_2|^n\right)^{1/n} .$$

This expression has the form of an L^p norm which is defined as

$$\|x\|_p = \left(|x_1|^p + |x_2|^p + \cdots + |x_n|^p\right)^{1/p} .$$

When $p = \infty$, the we get the L^∞ norm,

$\|x\|_\infty = \max\{|x_1|, |x_2|, \ldots, |x_n|\}$. Comparing this with the Hosford criterion

indicates that if $n = \infty$, we have

$$(\sigma_y)_{n\to\infty} = \max\left(|\sigma_2 - \sigma_3|, |\sigma_3 - \sigma_1|, |\sigma_1 - \sigma_2|\right) .$$

This is identical to the Tresca yield criterion.

Therefore, when *n = 1* or *n* goes to infinity the Hosford criterion reduces to the Tresca yield criterion. When *n = 2* the Hosford criterion reduces to the von Mises yield criterion.

Note that the exponent *n* does not need to be an integer.

Hosford yield criterion for plane stress

For the practically important situation of plane stress, the Hosford yield criterion takes the form

$$\frac{1}{2}\left(|\sigma_1|^n + |\sigma_2|^n\right) + \frac{1}{2}|\sigma_1 - \sigma_2|^n = \sigma_y^n$$

A plot of the yield locus in plane stress for various values of the exponent $n \geq 1$is shown in the adjacent figure.

Logan-Hosford yield criterion for anisotropic plasticity

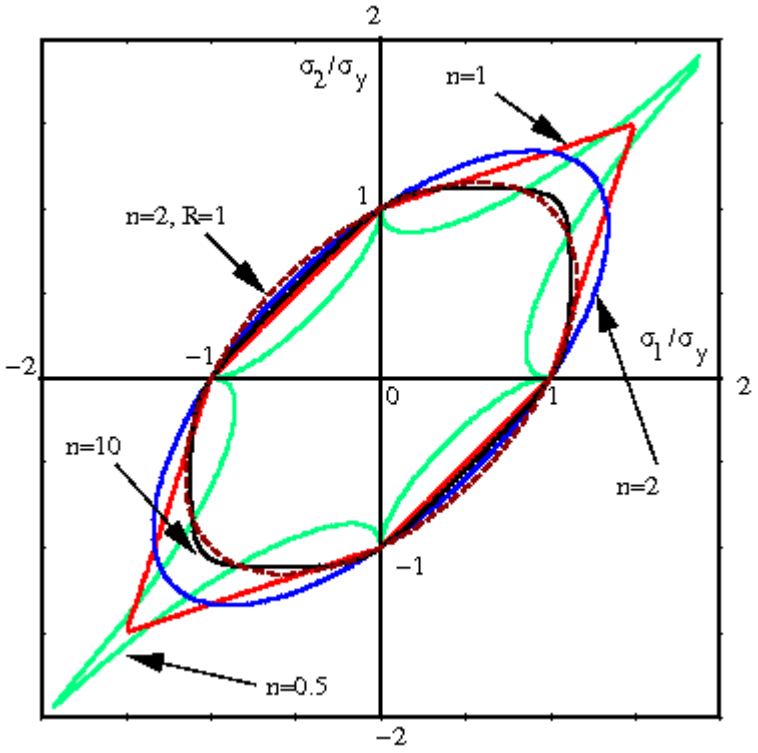

The plane stress, anisotropic, Hosford yield surface for four values of *n* and R=2.0

The Logan-Hosford yield criterion for anisotropic plasticity is similar to Hill's generalized yield criterion and has the form

$$F|\sigma_2 - \sigma_3|^n + G|\sigma_3 - \sigma_1|^n + H|\sigma_1 - \sigma_2|^n = 1$$

where *F,G,H* are constants, σ_i are the principal stresses, and the exponent *n* depends on the type of crystal (bcc, fcc, hcp, etc.) and has a value much greater than 2. Accepted values of *n* are 6 for bcc materials and 8 for fcc materials.

Though the form is similar to Hill's generalized yield criterion, the exponent *n* is independent of the R-value unlike the Hill's criterion.

Logan-Hosford criterion in plane stress

Under plane stress conditions, the Logan-Hosford criterion can be expressed as

$$\frac{1}{1+R}(|\sigma_1|^n + |\sigma_2|^n) + \frac{R}{1+R}|\sigma_1 - \sigma_2|^n = \sigma_y^n$$

where *R* is the R-value and σ_y is the yield stress in uniaxial tension/compression. For a derivation of this relation see Hill's yield criteria for plane stress. A plot of the yield locus

for the anisotropic Hosford criterion is shown in the adjacent figure. For values of n that are less than 2, the yield locus exhibits corners and such values are not recommended.

Chapter 3

Mohr–Coulomb Theory

Mohr–Coulomb theory is a mathematical model describing the response of brittle materials such as concrete, or rubble piles, to shear stress as well as normal stress. Most of the classical engineering materials somehow follow this rule in at least a portion of their shear failure envelope. Generally the theory applies to materials for which the compressive strength far exceeds the tensile strength.

In Geotechnical Engineering it is used to define shear strength of soils and rocks at different effective stresses.

In structural engineering it is used to determine failure load as well as the angle of fracture of a displacement fracture in concrete and similar materials. Coulomb's friction hypothesis is used to determine the combination of shear and normal stress that will cause a fracture of the material. Mohr's circle is used to determine which principal stresses that will produce this combination of shear and normal stress, and the angle of the plane in which this will occur. According to the principle of normality the stress introduced at failure will be perpendicular to the line describing the fracture condition.

It can be shown that a material failing according to Coulomb's friction hypothesis will show the displacement introduced at failure forming an angle to the line of fracture equal to the angle of friction. This makes the strength of the material determinable by comparing the external mechanical work introduced by the displacement and the external load with the internal mechanical work introduced by the strain and stress at the line of failure. By conservation of energy the sum of these must be zero and this will make it possible to calculate the failure load of the construction.

A common improvement of this model is to combine Coulomb's friction hypothesis with Rankine's principal stress hypothesis to describe a separation fracture.

History of the development

The Mohr–Coulomb theory is named in honour of Charles-Augustin de Coulomb and Christian Otto Mohr. Coulomb's contribution was a 1776 essay entitled "*Essai sur une application des règles des maximis et minimis à quelques problèmes de statique relatifs à l'architecture*" . Mohr developed a generalised form of the theory around the end of the 19th century. As the generalised form affected the interpretation of the criterion, but not the substance of it, some texts continue to refer to the criterion as simply the **'Coulomb criterion'** .

Mohr–Coulomb failure criterion

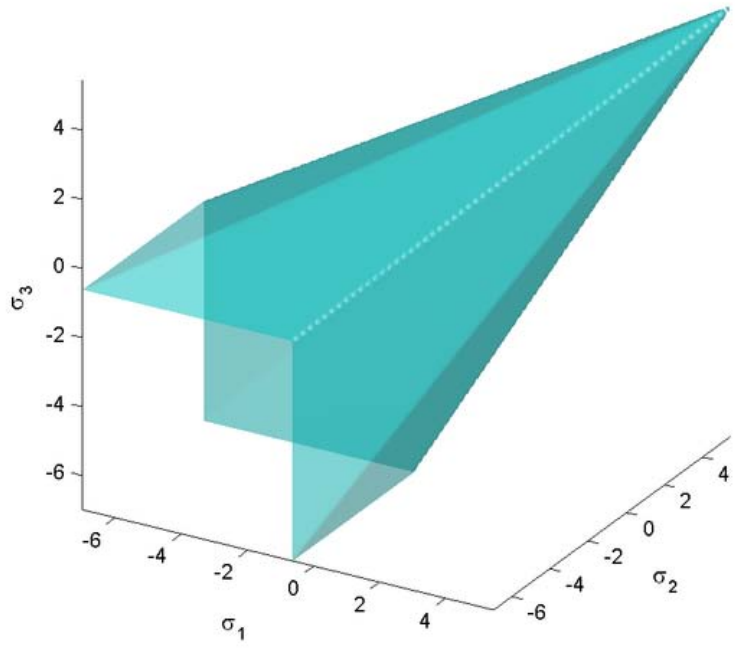

Figure 1: View of Mohr–Coulomb failure surface in 3D space of principal stresses for $c = 2, \phi = -20^\circ$

The Mohr–Coulomb failure criterion represents the linear envelope that is obtained from a plot of the shear strength of a material versus the applied normal stress. This relation is expressed as

$$\tau = \sigma \ \tan(\phi) + c$$

where τ is the shear strength, σ is the normal stress, *c* is the intercept of the failure envelope with the τ axis, and φ is the slope of the failure envelope. The quantity *c* is often called the **cohesion** and the angle φ is called the **angle of internal friction** . Compression is assumed to be positive in the following discussion. If compression is assumed to be negative then σ should be replaced with − σ.

If φ = 0, the Mohr–Coulomb criterion reduces to the Tresca criterion. On the other hand, if $\phi = 90^\circ$ the Mohr–Coulomb model is equivalent to the Rankine model. Higher values of φ are not allowed.

From Mohr's circle we have

$$\sigma = \sigma_m - \tau_m \sin\phi \ ; \quad \tau = \tau_m \cos\phi$$

where

$$\tau_m = \frac{\sigma_1 - \sigma_3}{2} \ ; \quad \sigma_m = \frac{\sigma_1 + \sigma_3}{2}$$

and σ_1 is the maximum principal stress and σ_3 is the minimum principal stress.

Therefore the Mohr–Coulomb criterion may also be expressed as

$$\tau_m = \sigma_m \sin\phi + c\cos\phi \ .$$

This form of the Mohr–Coulomb criterion is applicable to failure on a plane that is parallel to the σ_2 direction.

Mohr–Coulomb failure criterion in three dimensions

The Mohr–Coulomb criterion in three dimensions is often expressed as

$$\begin{cases} \pm\dfrac{\sigma_1 - \sigma_2}{2} = \left[\dfrac{\sigma_1 + \sigma_2}{2}\right]\sin(\phi) + c\cos(\phi) \\ \pm\dfrac{\sigma_2 - \sigma_3}{2} = \left[\dfrac{\sigma_2 + \sigma_3}{2}\right]\sin(\phi) + c\cos(\phi) \\ \pm\dfrac{\sigma_3 - \sigma_1}{2} = \left[\dfrac{\sigma_3 + \sigma_1}{2}\right]\sin(\phi) + c\cos(\phi) \end{cases}$$

The Mohr–Coulomb failure surface is a cone with a hexagonal cross section in deviatoric stress space.

The expressions for τ and σ can be generalized to three dimensions by developing expressions for the normal stress and the resolved shear stress on a plane of arbitrary orientation with respect to the coordinate axes (basis vectors). If the unit normal to the plane of interest is

$$\mathbf{n} = n_1\ \mathbf{e}_1 + n_2\ \mathbf{e}_2 + n_3\ \mathbf{e}_3$$

where $\mathbf{e}_i, \quad i = 1, 2, 3$ are three orthonormal unit basis vectors, and if the principal stresses $\sigma_1,\sigma_2,\sigma_3$ are aligned with the basis vectors $\mathbf{e}_1, \mathbf{e}_2, \mathbf{e}_3$, then the expressions for σ,τ are

$$\begin{aligned}\sigma &= n_1^2\sigma_1 + n_2^2\sigma_2 + n_3^2\sigma_3 \\ \tau &= \sqrt{(n_1\sigma_1)^2 + (n_2\sigma_2)^2 + (n_3\sigma_3)^2 - \sigma^2} \\ &= \sqrt{n_1^2n_2^2(\sigma_1 - \sigma_2)^2 + n_2^2n_3^2(\sigma_2 - \sigma_3)^2 + n_3^2n_1^2(\sigma_3 - \sigma_1)^2}\end{aligned}$$

The Mohr–Coulomb failure criterion can then be evaluated using the usual expression

$$\tau = \sigma\ \tan(\phi) + c$$

for the six planes of maximum shear stress.

Derivation of normal and shear stress on a plane

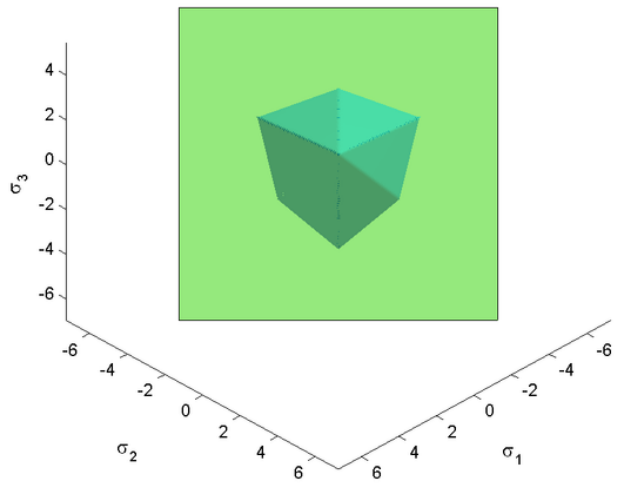

Figure 2: Mohr–Coulomb yield surface in the π-plane for $c = 2, \phi = -20°$

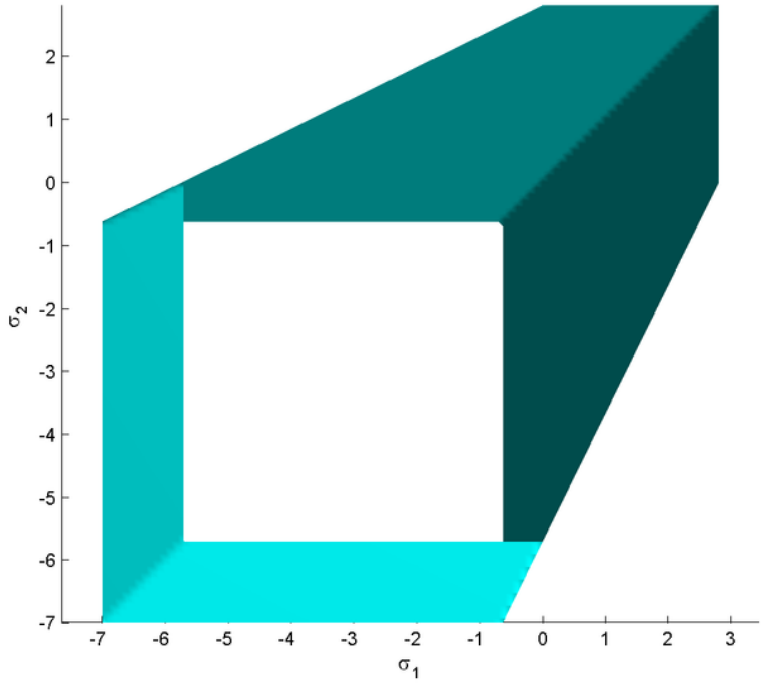

Figure 3: Trace of the Mohr–Coulomb yield surface in the $\sigma_1 - \sigma_2$-plane for $c = 2, \phi = -20^\circ$

Mohr–Coulomb failure surface in Haigh–Westergaard space

The Mohr–Coulomb failure (yield) surface is often expressed in Haigh–Westergaad coordinates. For example, the function

$$\frac{\sigma_1 - \sigma_3}{2} = \frac{\sigma_1 + \sigma_3}{2} \sin\phi + c\cos\phi$$

can be expressed as

$$\left[\sqrt{3}\ \sin\left(\theta + \frac{\pi}{3}\right) - \sin\phi\cos\left(\theta + \frac{\pi}{3}\right)\right]\rho - \sqrt{2}\sin(\phi)\xi = \sqrt{6}c\cos\phi$$

Alternatively, in terms of the invariants *p*,*q*,*r* we can write

$$\left[\frac{1}{\sqrt{3}\ \cos\phi}\ \sin\left(\theta + \frac{\pi}{3}\right) - \frac{1}{3}\tan\phi\ \cos\left(\theta + \frac{\pi}{3}\right)\right]q - p\ \tan\phi = c$$

where

$$\theta = \frac{1}{3}\arccos\left[\left(\frac{r}{q}\right)^3\right] \quad .$$

Mohr–Coulomb yield and plasticity

The Mohr–Coulomb yield surface is often used to model the plastic flow of geomaterials (and other cohesive-frictional materials). Many such materials show dilatational behavior under triaxial states of stress which the Mohr–Coulomb model does not include. Also, since the yield surface has corners, it may be inconvenient to use the original Mohr–Coulomb model to determine the direction of plastic flow (in the flow theory of plasticity).

A common approach that is used is to use a **non-associated** plastic flow potential that is smooth. An example of such a potential is the function

$$g := \sqrt{(\alpha c_{\mathrm{y}} \tan\psi)^2 + G^2(\phi,\theta)\ q^2} - p\tan\phi$$

where α is a parameter, c_{y} is the value of c when the plastic strain is zero (also called the **initial cohesion yield stress**), ψ is the angle made by the yield surface in the **Rendulic plane** at high values of p (this angle is also called the **dilation angle**), and $G(\varphi,\theta)$ is an appropriate function that is also smooth in the deviatoric stress plane.

Chapter 4

Drucker Prager Yield Criterion

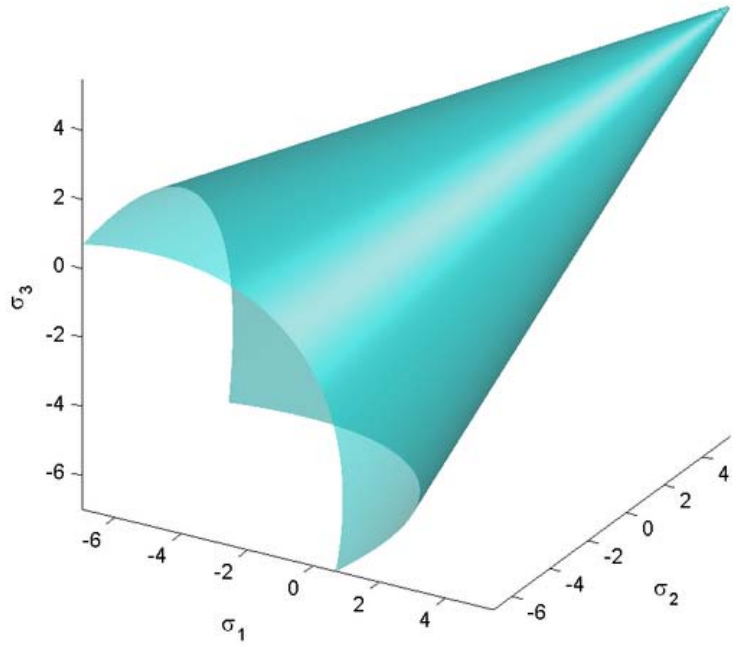

Figure 1: View of Drucker–Prager yield surface in 3D space of principal stresses for $c = 2, \phi = -20^\circ$

The Drucker–Prager yield criterion is a pressure-dependent model for determining whether a material has failed or undergone plastic yielding. The criterion was introduced to deal with the plastic deformation of soils. It and its many variants have been applied to rock, concrete, polymers, foams, and other pressure-dependent materials.

The Drucker–Prager yield criterion has the form

$$\sqrt{J_2} = A + B\ I_1$$

where I_1 is the first invariant of the Cauchy stress and J_2 is the second invariant of the deviatoric part of the Cauchy stress. The constants A,B are determined from experiments.

In terms of the equivalent stress (or von Mises stress) and the hydrostatic (or mean) stress, the Drucker–Prager criterion can be expressed as

$$\sigma_e = a + b\ \sigma_m$$

where σ_e is the equivalent stress, σ_m is the hydrostatic stress, and a,b are material constants. The Drucker–Prager yield criterion expressed in Haigh–Westergaard coordinates is

$$\tfrac{1}{\sqrt{2}}\rho - \sqrt{3}\ B\xi = A$$

The Drucker–Prager yield surface is a smooth version of the Mohr–Coulomb yield surface.

Expressions for A and B

The Drucker–Prager model can be written in terms of the principal stresses as

$$\sqrt{\frac{1}{6}[(\sigma_1 - \sigma_2)^2 + (\sigma_2 - \sigma_3)^2 + (\sigma_3 - \sigma_1)^2]} = A + B\ (\sigma_1 + \sigma_2 + \sigma_3)\ .$$

If σ_t is the yield stress in uniaxial tension, the Drucker–Prager criterion implies

$$\frac{1}{\sqrt{3}}\,\sigma_t = A + B\ \sigma_t\ .$$

If σ_c is the yield stress in uniaxial compression, the Drucker–Prager criterion implies

$$\frac{1}{\sqrt{3}}\,\sigma_c = A - B\ \sigma_c\ .$$

Solving these two equations gives

$$A = \frac{2}{\sqrt{3}}\ \left(\frac{\sigma_c\ \sigma_t}{\sigma_c + \sigma_t}\right)\ ;\quad B = \frac{1}{\sqrt{3}}\ \left(\frac{\sigma_t - \sigma_c}{\sigma_c + \sigma_t}\right)\ .$$

Uniaxial asymmetry ratio

Different uniaxial yield stresses in tension and in compression are predicted by the Drucker–Prager model. The uniaxial asymmetry ratio for the Drucker–Prager model is

$$\beta = \frac{\sigma_{\mathrm{c}}}{\sigma_{\mathrm{t}}} = \frac{1 - \sqrt{3}\ B}{1 + \sqrt{3}\ B}\ .$$

Expressions in terms of cohesion and friction angle

Since the Drucker–Prager yield surface is a smooth version of the Mohr–Coulomb yield surface, it is often expressed in terms of the cohesion (*c*) and the angle of internal friction (φ) that are used to describe the Mohr–Coulomb yield surface. If we assume that the Drucker–Prager yield surface **circumscribes** the Mohr–Coulomb yield surface then the expressions for *A* and *B* are

$$A = \frac{6\ c\ \cos\phi}{\sqrt{3}(3 + \sin\phi)}\ ; \quad B = \frac{2\ \sin\phi}{\sqrt{3}(3 + \sin\phi)}$$

If the Drucker–Prager yield surface **inscribes** the Mohr–Coulomb yield surface then

$$A = \frac{6\ c\ \cos\phi}{\sqrt{3}(3 - \sin\phi)}\ ; \quad B = \frac{2\ \sin\phi}{\sqrt{3}(3 - \sin\phi)}$$

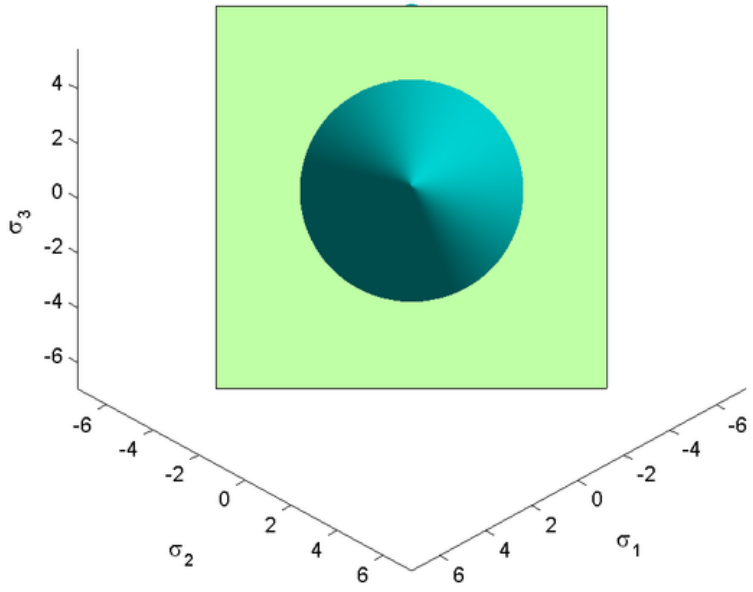

Figure 2: Drucker–Prager yield surface in the π-plane for $c = 2, \phi = -20^\circ$

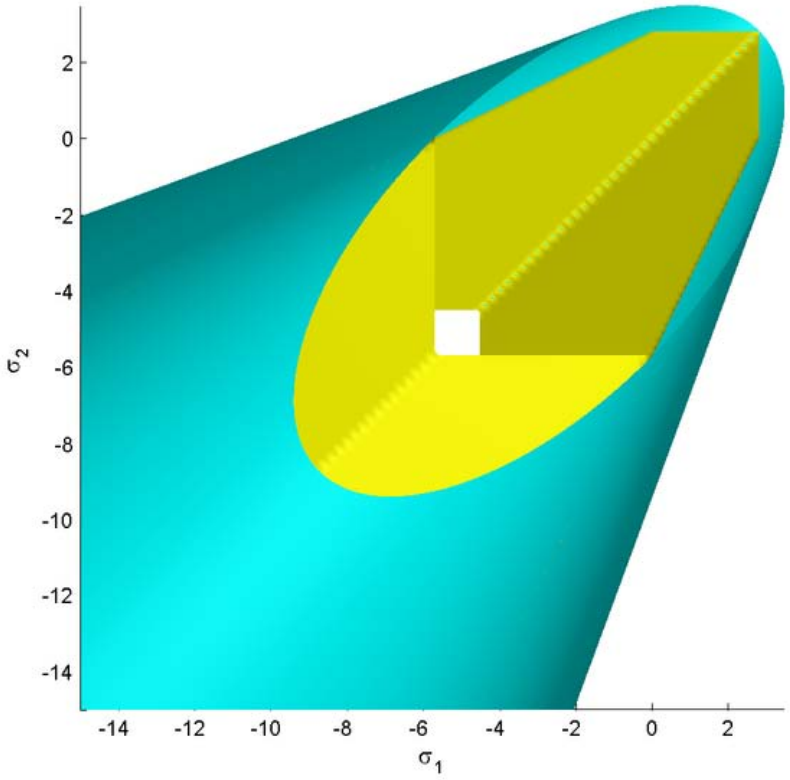

Figure 3: Trace of the Drucker–Prager and Mohr–Coulomb yield surfaces in the $\sigma_1 - \sigma_2$-plane for $c = 2, \phi = -20^\circ$. Yellow = Mohr–Coulomb, Cyan = Drucker–Prager.

Drucker–Prager model for polymers

The Drucker–Prager model has been used to model polymers such as polyoxymethylene and polypropylene. For polyoxymethylene the yield stress is a linear function of the pressure. However, polypropylene shows a quadratic pressure-dependence of the yield stress.

Drucker–Prager model for foams

For foams, the GAZT model uses

$$A = \pm \frac{\sigma_y}{\sqrt{3}}; \quad B = \mp \frac{1}{\sqrt{3}} \left(\frac{\rho}{5\ \rho_s} \right)$$

where σ_y is a critical stress for failure in tension or compression, ρ is the density of the foam, and ρ_s is the density of the base material.

Extensions of the isotropic Drucker–Prager model

The Drucker–Prager criterion can also be expressed in the alternative form

$$J_2 = (A + B\ I_1)^2 = a + b\ I_1 + c\ I_1^2\ .$$

Deshpande–Fleck yield criterion

The Deshpande–Fleck yield criterion for foams has the form given in above equation. The parameters *a*,*b*,*c* for the Deshpande–Fleck criterion are

$$a = (1 + \beta^2)\ \sigma_y^2\ , \quad b = 0\ , \quad c = -\frac{\beta^2}{3}$$

where β is a parameter that determines the shape of the yield surface, and σ_y is the yield stress in tension or compression.

Anisotropic Drucker–Prager yield criterion

An anisotropic form of the Drucker–Prager yield criterion is the Liu–Huang–Stout yield criterion . This yield criterion is an extension of the generalized Hill yield criterion and has the form

$$\begin{aligned} f :=& \sqrt{F(\sigma_{11}-\sigma_{22})^2 + G(\sigma_{22}-\sigma_{33})^2 + H(\sigma_{33}-\sigma_{11})^2 + 2L\sigma_{23}^2 + 2M\sigma_{31}^2 + 2N\sigma_{12}^2} \\ &+ I\sigma_{11} + J\sigma_{22} + K\sigma_{33} - 1 \le 0 \end{aligned}$$

The coefficients *F*,*G*,*H*,*L*,*M*,*N*,*I*,*J*,*K* are

$$\begin{aligned} F =& \frac{1}{2}\left[\Sigma_2^2 + \Sigma_3^2 - \Sigma_1^2\right]\ ;\quad G = \frac{1}{2}\left[\Sigma_3^2 + \Sigma_1^2 - \Sigma_2^2\right]\ ;\quad H = \frac{1}{2}\left[\Sigma_1^2 + \Sigma_2^2 - \Sigma_3^2\right] \\ L =& \frac{1}{2(\sigma_{23}^y)^2}\ ;\quad M = \frac{1}{2(\sigma_{31}^y)^2}\ ;\quad N = \frac{1}{2(\sigma_{12}^y)^2} \\ I =& \frac{\sigma_{1c} - \sigma_{1t}}{2\sigma_{1c}\sigma_{1t}}\ ;\quad J = \frac{\sigma_{2c} - \sigma_{2t}}{2\sigma_{2c}\sigma_{2t}}\ ;\quad K = \frac{\sigma_{3c} - \sigma_{3t}}{2\sigma_{3c}\sigma_{3t}} \end{aligned}$$

where

$$\Sigma_1 := \frac{\sigma_{1c} + \sigma_{1t}}{2\sigma_{1c}\sigma_{1t}}\ ;\quad \Sigma_2 := \frac{\sigma_{2c} + \sigma_{2t}}{2\sigma_{2c}\sigma_{2t}}\ ;\quad \Sigma_3 := \frac{\sigma_{3c} + \sigma_{3t}}{2\sigma_{3c}\sigma_{3t}}$$

and $\sigma_{ic}, i = 1,2,3$ are the uniaxial yield stresses in **compression** in the three principal directions of anisotropy, $\sigma_{it}, i = 1,2,3$ are the uniaxial yield stresses in **tension**, and $\sigma_{23}^{y}, \sigma_{31}^{y}, \sigma_{12}^{y}$ are the yield stresses in pure shear.

The Drucker yield criterion

The Drucker–Prager criterion should not be confused with the earlier Drucker criterion which is independent of the pressure (I_1). The Drucker yield criterion has the form

$$f := J_2^3 - \alpha\ J_3^2 - k^2 \leq 0$$

where J_2 is the second invariant of the deviatoric stress, J_3 is the third invariant of the deviatoric stress, α is a constant that lies between -27/8 and 9/4 (for the yield surface to be convex), k is a constant that varies with the value of α. For α = 0, $k^2 = \frac{\sigma_y^6}{27}$ where σ_y is the yield stress in uniaxial tension.

Anisotropic Drucker Criterion

An anisotropic version of the Drucker yield criterion is the Cazacu–Barlat (CZ) yield criterion which has the form

$$f := (J_2^0)^3 - \alpha\ (J_3^0)^2 - k^2 \leq 0$$

where J_2^0, J_3^0 are generalized forms of the deviatoric stress and are defined as

$$J_2^0 := \frac{1}{6}\left[a_1(\sigma_{22}-\sigma_{33})^2 + a_2(\sigma_{33}-\sigma_{11})^2 + a_3(\sigma_{11}-\sigma_{22})^2\right] + a_4\sigma_{23}^2 + a_5\sigma_{31}^2 + a_6\sigma_{12}^2$$

$$\begin{aligned} J_3^0 :=& \frac{1}{27}\left[(b_1+b_2)\sigma_{11}^3 + (b_3+b_4)\sigma_{22}^3 + \{2(b_1+b_4)-(b_2+b_3)\}\sigma_{33}^3\right] \\ & - \frac{1}{9}\left[(b_1\sigma_{22}+b_2\sigma_{33})\sigma_{11}^2 + (b_3\sigma_{33}+b_4\sigma_{11})\sigma_{22}^2 + \{(b_1-b_2+b_4)\sigma_{11}+(b_1-b_3+b_4)\sigma_{22}\}\sigma_{33}^2\right] \\ & + \frac{2}{9}(b_1+b_4)\sigma_{11}\sigma_{22}\sigma_{33} + 2b_{11}\sigma_{12}\sigma_{23}\sigma_{31} \\ & - \frac{1}{3}\left[\{2b_9\sigma_{22} - b_8\sigma_{33} - (2b_9-b_8)\sigma_{11}\}\sigma_{31}^2 + \{2b_{10}\sigma_{33} - b_5\sigma_{22} - (2b_{10}-b_5)\sigma_{11}\}\sigma_{12}^2 \right. \\ & \left. \{(b_6+b_7)\sigma_{11} - b_6\sigma_{22} - b_7\sigma_{33}\}\sigma_{23}^2\right] \end{aligned}$$

Cazacu–Barlat yield criterion for plane stress

For thin sheet metals, the state of stress can be approximated as plane stress. In that case the Cazacu–Barlat yield criterion reduces to its two-dimensional version with

$$J_2^0 = \frac{1}{6}\left[(a_2+a_3)\sigma_{11}^2 + (a_1+a_3)\sigma_{22}^2 - 2a_3\sigma_1\sigma_2\right] + a_6\sigma_{12}^2$$

$$J_3^0 = \frac{1}{27}\left[(b_1+b_2)\sigma_{11}^3 + (b_3+b_4)\sigma_{22}^3\right] - \frac{1}{9}\left[b_1\sigma_{11} + b_4\sigma_{22}\right]\sigma_{11}\sigma_{22} + \frac{1}{3}\left[b_5\sigma_{22} + (2b_{10}-b_5)\sigma_{11}\right]\sigma_{12}^2$$

For thin sheets of metals and alloys, the parameters of the Cazacu–Barlat yield criterion are

Table 1. **Cazacu–Barlat yield criterion parameters for sheet metals and alloys**

Material	a_1	a_2	a_3	a_6	b_1	b_2	b_3	b_4	b_5	b_{10}	α
6016-T4 Aluminum Alloy	0.815	0.815	0.334	0.42	0.04	-1.205	-0.958	0.306	0.153	-0.02	1.4
2090-T3 Aluminum Alloy	1.05	0.823	0.586	0.96	1.44	0.061	-1.302	-0.281	-0.375	0.445	1.285

Chapter 5

Bresler Pister Yield Criterion

The **Bresler-Pister yield criterion** is a function that was originally devised to predict the strength of concrete under multiaxial stress states. This yield criterion is an extension of the Drucker-Prager yield criterion and can be expressed on terms of the stress invariants as

$$\sqrt{J_2} = A + B\ I_1 + C\ I_1^2$$

where I_1 is the first invariant of the Cauchy stress, J_2 is the second invariant of the deviatoric part of the Cauchy stress, and A,B,C are material constants.

Yield criteria of this form have also been used for polypropylene and polymeric foams .

The parameters A,B,C have to be chosen with care for reasonably shaped yield surfaces. If σ_c is the yield stress in uniaxial compression, σ_t is the yield stress in uniaxial tension, and σ_b is the yield stress in biaxial compression, the parameters can be expressed as

$$B = \left(\frac{\sigma_t - \sigma_c}{\sqrt{3}(\sigma_t + \sigma_c)}\right)\left(\frac{4\sigma_b^2 - \sigma_b(\sigma_c + \sigma_t) + \sigma_c\sigma_t}{4\sigma_b^2 + 2\sigma_b(\sigma_t - \sigma_c) - \sigma_c\sigma_t}\right)$$

$$C = \left(\frac{1}{\sqrt{3}(\sigma_t + \sigma_c)}\right)\left(\frac{\sigma_b(3\sigma_t - \sigma_c) - 2\sigma_c\sigma_t}{4\sigma_b^2 + 2\sigma_b(\sigma_t - \sigma_c) - \sigma_c\sigma_t}\right)$$

$$A = \frac{\sigma_c}{\sqrt{3}} + c_1\sigma_c - c_2\sigma_c^2$$

Derivation of expressions for parameters A, B, C

The Bresler-Pister yield criterion in terms of the principal stresses $\sigma_1,\sigma_2,\sigma_3$ is

$$\frac{1}{\sqrt{6}}\left[(\sigma_1-\sigma_2)^2+(\sigma_2-\sigma_3)^2+(\sigma_3-\sigma_1)^2\right]^{1/2}-A-B\,(\sigma_1+\sigma_2+\sigma_3)-C\,(\sigma_1+\sigma_2+\sigma_3)^2=0\,.$$

If $\sigma_t = \sigma_1$ is the yield stress in uniaxial tension, then

$$\frac{1}{\sqrt{3}}\,\sigma_t - A - B\sigma_t - C\sigma_t^2 = 0\ .$$

If $-\sigma_c = \sigma_1$ is the yield stress in uniaxial compression, then

$$\frac{1}{\sqrt{3}}\,\sigma_c - A + B\sigma_c - C\sigma_c^2 = 0\ .$$

If $-\sigma_b = \sigma_1 = \sigma_2$ is the yield stress in equibiaxial compression, then

$$\frac{1}{\sqrt{3}}\,\sigma_b - A + 2B\sigma_b - 4C\sigma_b^2 = 0\ .$$

Solving these three equations for A,B,C (using Maple) gives us

$$A := \frac{1}{\sqrt{3}}\,\frac{\sigma_c\sigma_t\sigma_b(\sigma_t+8\sigma_b-3\sigma_c)}{(\sigma_c+\sigma_t)(2\sigma_b-\sigma_c)(2\sigma_b+\sigma_t)}$$

$$B := \frac{1}{\sqrt{3}}\,\frac{(\sigma_c-\sigma_t)(\sigma_b\sigma_c+\sigma_b\sigma_t-\sigma_c\sigma_t-4\sigma_b^2)}{(\sigma_c+\sigma_t)(2\sigma_b-\sigma_c)(2\sigma_b+\sigma_t)}$$

$$C := \frac{1}{\sqrt{3}}\,\frac{3\sigma_b\sigma_t-\sigma_b\sigma_c-2\sigma_c\sigma_t}{(\sigma_c+\sigma_t)(2\sigma_b-\sigma_c)(2\sigma_b+\sigma_t)}$$

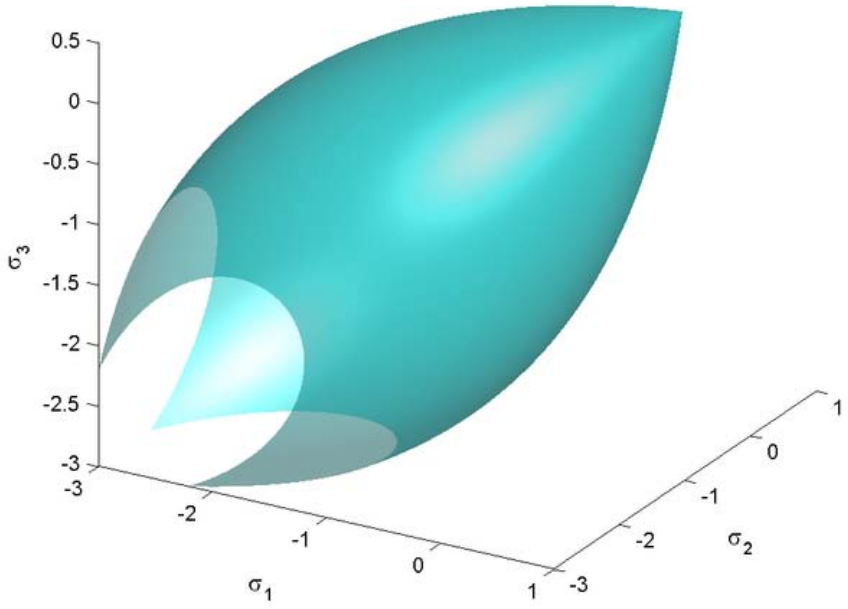

Figure 1: View of the three-parameter Bresler-Pister yield surface in 3D space of principal stresses for $\sigma_c = 1, \sigma_t = 0.3, \sigma_b = 1.7$

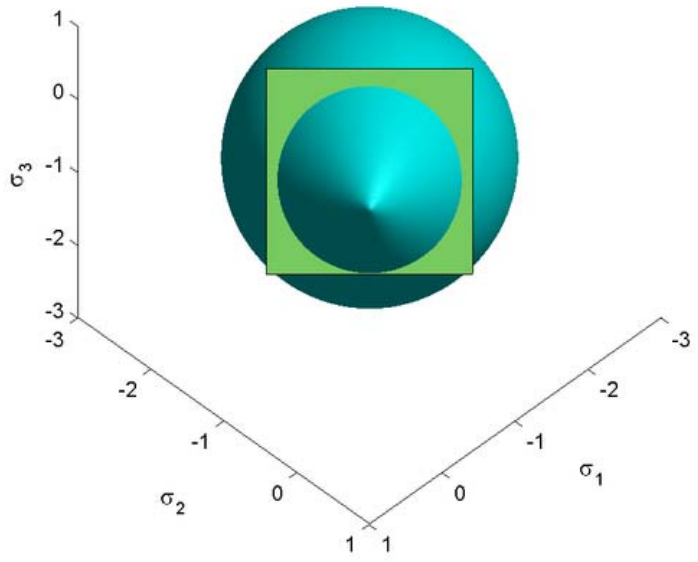

Figure 2: The three-parameter Bresler-Pister yield surface in the π-plane for $\sigma_c = 1, \sigma_t = 0.3, \sigma_b = 1.7$

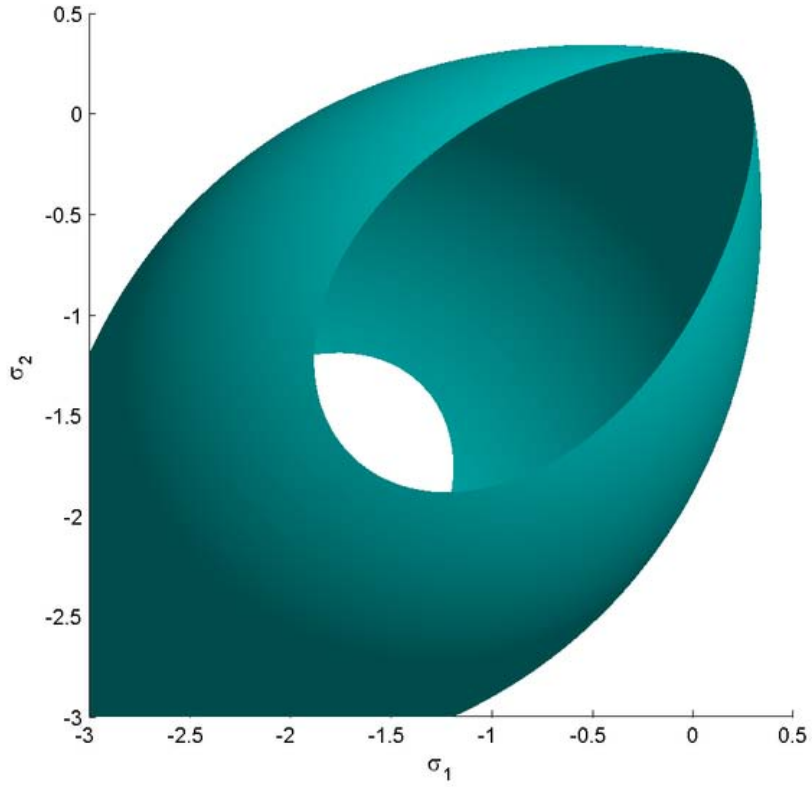

Figure 3: Trace of the three-parameter Bresler-Pister yield surface in the $\sigma_1 - \sigma_2$-plane for $\sigma_c = 1, \sigma_t = 0.3, \sigma_b = 1.7$

Alternative forms of the Bresler-Pister yield criterion

In terms of the equivalent stress (σ_e) and the mean stress (σ_m), the Bresler-Pister yield criterion can be written as

$$\sigma_e = a + b\,\sigma_m + c\,\sigma_m^2\;; \quad \sigma_e = \sqrt{3J_2}\;, \quad \sigma_m = I_1/3\;.$$

The Etse-Willam form of the Bresler-Pister yield criterion for concrete can be expressed as

$$\sqrt{J_2} = \frac{1}{\sqrt{3}}\,I_1 - \frac{1}{2\sqrt{3}}\left(\frac{\sigma_t}{\sigma_c^2 - \sigma_t^2}\right)\,I_1^2$$

where σ_c is the yield stress in uniaxial compression and σ_t is the yield stress in uniaxial tension.

The GAZT yield criterion for plastic collapse of foams also has a form similar to the Bresler-Pister yield criterion and can be expressed as

$$\sqrt{J_2} = \begin{cases} \frac{1}{\sqrt{3}}\,\sigma_t - 0.03\sqrt{3}\frac{\rho}{\rho_m\ \sigma_t}\ I_1^2 \\ -\frac{1}{\sqrt{3}}\,\sigma_c + 0.03\sqrt{3}\frac{\rho}{\rho_m\ \sigma_c}\ I_1^2 \end{cases}$$

where ρ is the density of the foam and ρ_m is the density of the matrix material.

Chapter 6

Willam-Warnke Yield Criterion

The **Willam-Warnke yield criterion** is a function that is used to predict when failure will occur in concrete and other cohesive-frictional materials such as rock, soil, and ceramics. This yield criterion has the functional form

$$f(I_1, J_2, J_3) = 0$$

where I_1 is the first invariant of the Cauchy stress tensor, and J_2,J_3 are the second and third invariants of the deviatoric part of the Cauchy stress tensor. There are three material parameters (σ_c - the uniaxial compressive strength, σ_t - the uniaxial tensile strength, σ_b - the equibiaxial compressive strength) that have to be determined before the Willam-Warnke yield criterion may be applied to predict failure.

In terms of I_1,J_2,J_3, the Willam-Warnke yield criterion can be expressed as

$$f := \sqrt{J_2} + \lambda(J_2, J_3)\ (\tfrac{I_1}{3} - B) = 0$$

where λ is a function that depends on J_2,J_3 and the three material parameters and B depends only on the material parameters. The function λ can be interpreted as the friction angle which depends on the Lode angle (θ). The quantity B is interpreted as a cohesion pressure. The Willam-Warnke yield criterion may therefore be viewed as a combination of the Mohr-Coulomb and the Drucker-Prager yield criteria.

Willam-Warnke yield function

In the original paper, the three-parameter Willam-Warnke yield function was expressed as

$$f := \frac{1}{3z}\frac{I_1}{\sigma_c} + \sqrt{\frac{2}{5}}\frac{1}{r(\theta)}\frac{\sqrt{J_2}}{\sigma_c} - 1 \leq 0$$

where I_1 is the first invariant of the stress tensor, J_2 is the second invariant of the deviatoric part of the stress tensor, σ_c is the yield stress in uniaxial compression, and θ is the Lode angle given by

$$\theta = \tfrac{1}{3}\cos^{-1}\left(\frac{3\sqrt{3}}{2}\frac{J_3}{J_2^{3/2}}\right) .$$

The locus of the boundary of the stress surface in the deviatoric stress plane is expressed in polar coordinates by the quantity $r(\theta)$ which is given by

$$r(\theta) := \frac{u(\theta) + v(\theta)}{w(\theta)}$$

where

$$u(\theta) := 2\, r_c\, (r_c^2 - r_t^2)\, \cos\theta$$
$$v(\theta) := r_c\, (2\, r_t - r_c)\sqrt{4\, (r_c^2 - r_t^2)\, \cos^2\theta + 5\, r_t^2 - 4\, r_t\, r_c}$$
$$w(\theta) := 4(r_c^2 - r_t^2)\cos^2\theta + (r_c - 2\, r_t)^2$$

The quantities r_t and r_c describe the position vectors at the locations $\theta = 0^\circ, 60^\circ$ and can be expressed in terms of σ_c,σ_b,σ_t as

$$r_c := \sqrt{\frac{6}{5}}\left[\frac{\sigma_b\sigma_t}{3\sigma_b\sigma_t + \sigma_c(\sigma_b - \sigma_t)}\right] \quad ; \quad r_t := \sqrt{\frac{6}{5}}\left[\frac{\sigma_b\sigma_t}{\sigma_c(2\sigma_b + \sigma_t)}\right]$$

The parameter z in the model is given by

$$z := \frac{\sigma_b\sigma_t}{\sigma_c(\sigma_b - \sigma_t)} .$$

The Haigh-Westergaard representation of the Willam-Warnke yield condition can be written as

$$f(\xi, \rho, \theta) = 0 \quad \equiv \quad f := \bar{\lambda}(\theta)\ \rho + \bar{B}\ \xi - \sigma_c \leq 0$$

where

$$\bar{B} := \frac{1}{\sqrt{3}\ z}\ ;\quad \bar{\lambda} := \frac{1}{\sqrt{5}\ r(\theta)}\ .$$

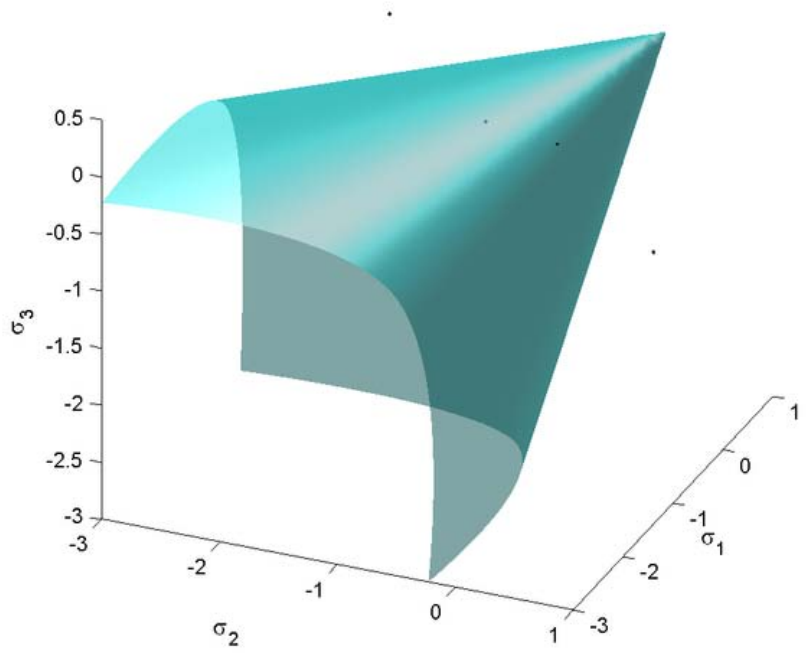

Figure 1: View of three-parameter Willam-Warnke yield surface in 3D space of principal stresses for $\sigma_c = 1, \sigma_t = 0.3, \sigma_b = 1.7$

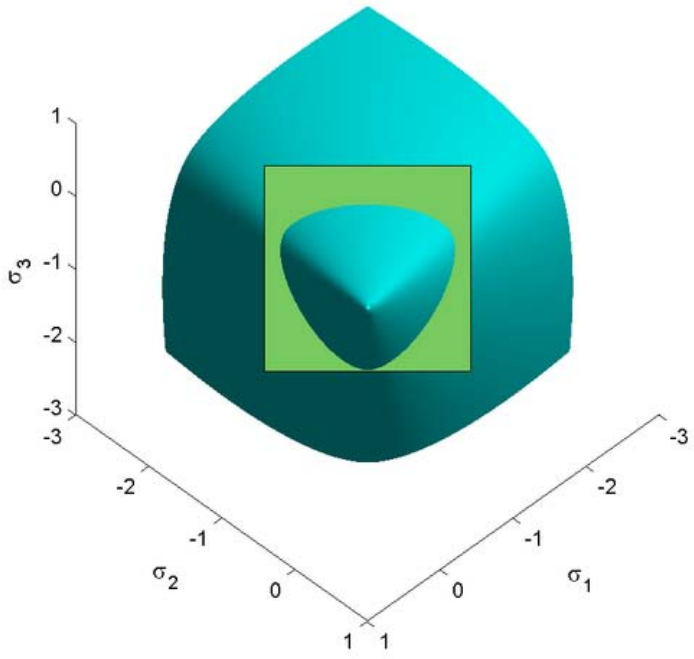

Figure 2: Three-parameter Willam-Warnke yield surface in the π-plane for $\sigma_c = 1, \sigma_t = 0.3, \sigma_b = 1.7$

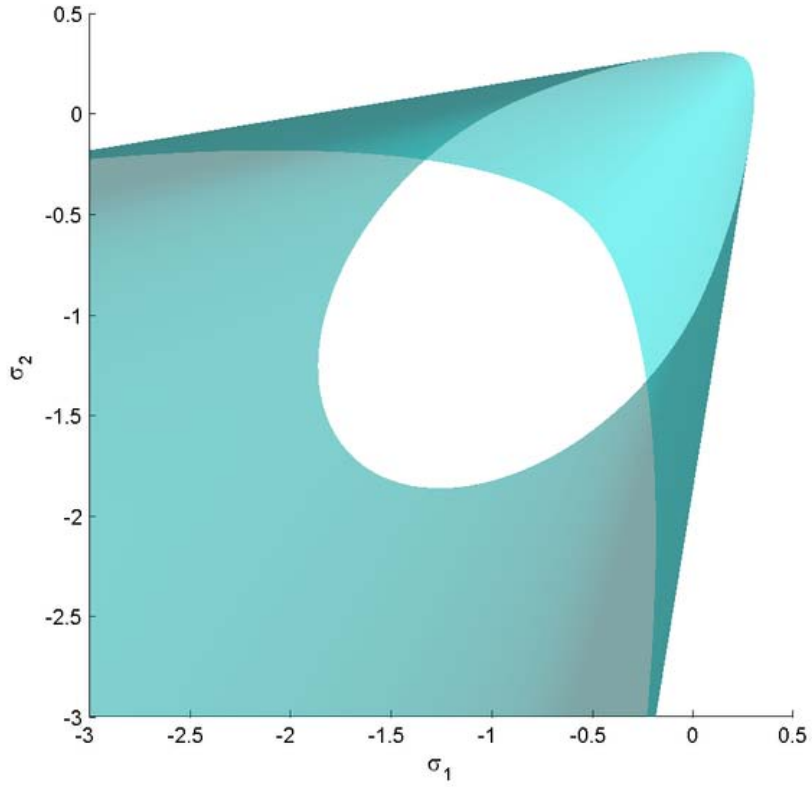

Figure 3: Trace of the three-parameter Willam-Warnke yield surface in the $\sigma_1 - \sigma_2$-plane for $\sigma_c = 1, \sigma_t = 0.3, \sigma_b = 1.7$

Modified forms of the Willam-Warnke yield criterion

An alternative form of the Willam-Warnke yield criterion in Haigh-Westergaard coordinates is the Ulm-Coussy-Bazant form :

$$f(\xi, \rho, \theta) = 0 \quad \text{or} \quad f := \rho + \bar{\lambda}(\theta) \ \left(\xi - \bar{B}\right) = 0$$

where

$$\bar{\lambda} := \sqrt{\tfrac{2}{3}} \ \frac{u(\theta) + v(\theta)}{w(\theta)} \ ; \quad \bar{B} := \tfrac{1}{\sqrt{3}} \ \left[\frac{\sigma_b \sigma_t}{\sigma_b - \sigma_t}\right]$$

and

$$r_t := \frac{\sqrt{3}\,(\sigma_b - \sigma_t)}{2\sigma_b - \sigma_t}$$

$$r_c := \frac{\sqrt{3}\,\sigma_c\,(\sigma_b - \sigma_t)}{(\sigma_c + \sigma_t)\sigma_b - \sigma_c\sigma_t}$$

The quantities r_c,r_t are interpreted as friction coefficients. For the yield surface to be convex, the Willam-Warnke yield criterion requires that $2\,r_t \geq r_c \geq r_t/2$and $0 \leq \theta \leq \frac{\pi}{3}$.

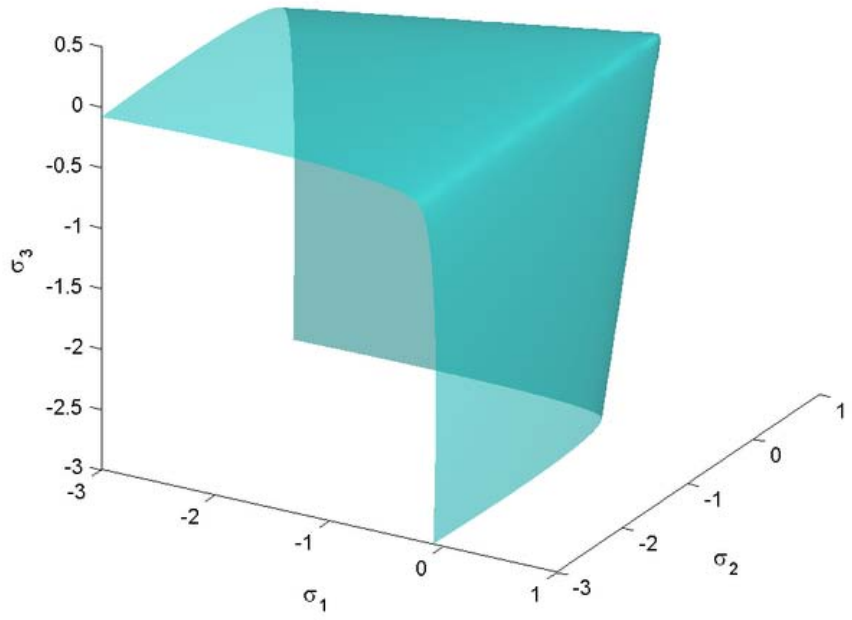

Figure 4: View of Ulm-Coussy-Bazant version of the three-parameter Willam-Warnke yield surface in 3D space of principal stresses for $\sigma_c = 1$,$\sigma_t = 0.3$,$\sigma_b = 1.7$

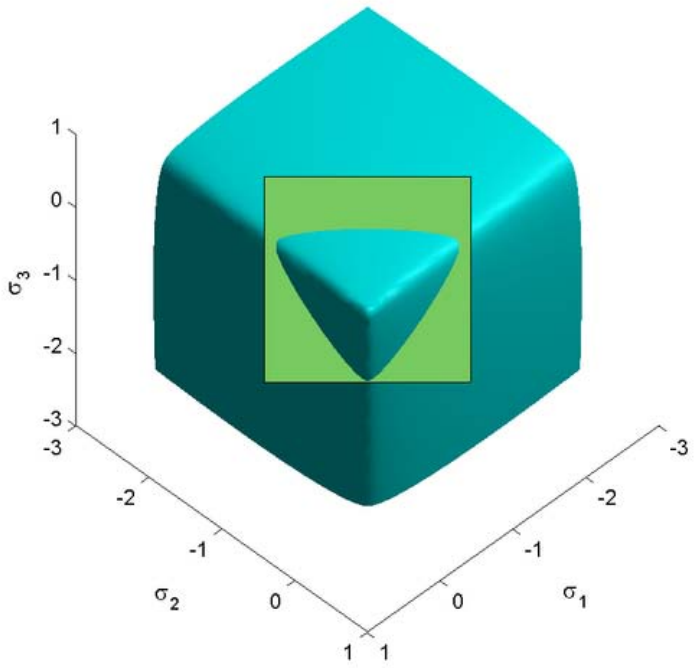

Figure 5: Ulm-Coussy-Bazant version of the three-parameter Willam-Warnke yield surface in the π-plane for $\sigma_c = 1, \sigma_t = 0.3, \sigma_b = 1.7$

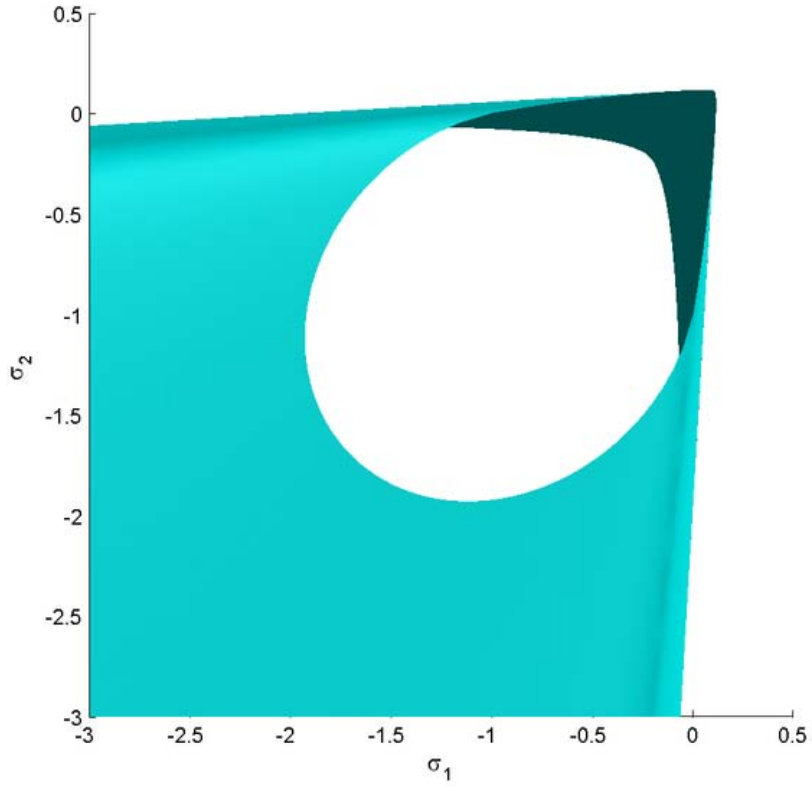

Figure 6: Trace of the Ulm-Coussy-Bazant version of the three-parameter Willam-Warnke yield surface in the $\sigma_1 - \sigma_2$-plane for $\sigma_c = 1, \sigma_t = 0.3, \sigma_b = 1.7$

Chapter 7

Grain Boundary Strengthening

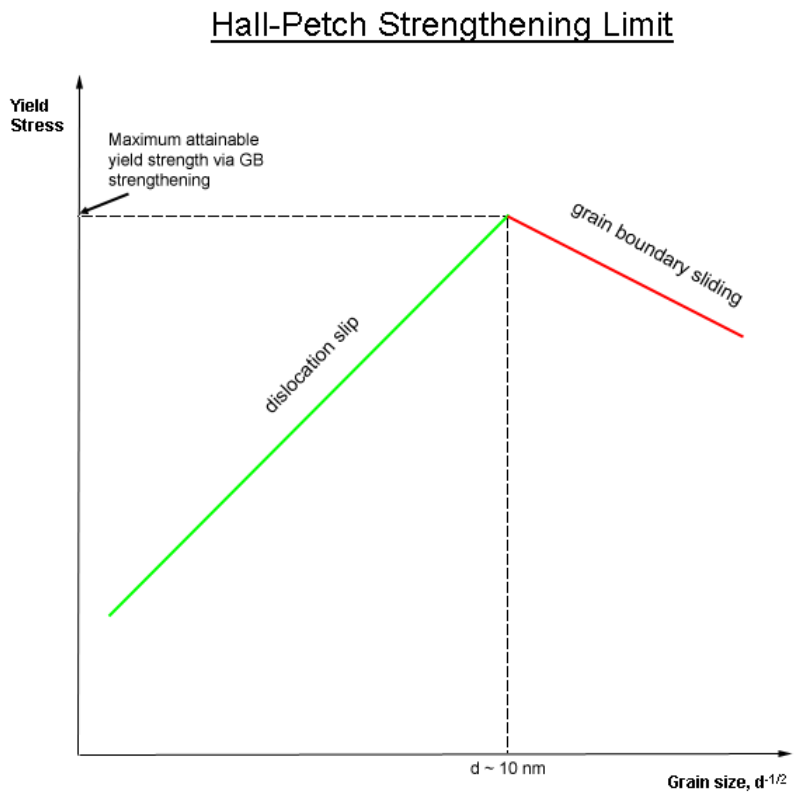

Figure 1: Hall-Petch Strengthening is limited by the size of dislocations. Once the grain size reaches about 10 nanometres (3.9×10^{-7} in), grain boundaries start to slide.

Grain-boundary strengthening (or **Hall-Petch strengthening**) is a method of strengthening materials by changing their average crystallite (grain) size. It is based on the observation that grain boundaries impede dislocation movement and that the number of dislocations within a grain have an effect on how easily dislocations can traverse grain boundaries and travel from grain to grain. So, by changing grain size one can influence

dislocation movement and yield strength. For example, heat treatment after plastic deformation and changing the rate of solidification are ways to alter grain size.

Theory

In grain-boundary strengthening the grain boundaries act as pinning points impeding further dislocation propagation. Since the lattice structure of adjacent grains differs in orientation, it requires more energy for a dislocation to change directions and move into the adjacent grain. The grain boundary is also much more disordered than inside the grain, which also prevents the dislocations from moving in a continuous slip plane. Impeding this dislocation movement will hinder the onset of plasticity and hence increase the yield strength of the material.

Under an applied stress, existing dislocations and dislocations generated by Frank-Read Sources will move through a crystalline lattice until encountering a grain boundary, where the large atomic mismatch between different grains creates a repulsive stress field to oppose continued dislocation motion. As more dislocations propagate to this boundary, dislocation 'pile up' occurs as a cluster of dislocations are unable to move past the boundary. As dislocations generate repulsive stress fields, each successive dislocation will apply a repulsive force to the dislocation incident with the grain boundary. These repulsive forces act as a driving force to reduce the energetic barrier for diffusion across the boundary, such that additional pile up causes dislocation diffusion across the grain boundary, allowing further deformation in the material. Decreasing grain size decreases the amount of possible pile up at the boundary, increasing the amount of applied stress necessary to move a dislocation across a grain boundary. The higher the applied stress to move the dislocation, the higher the yield strength. Thus, there is then an inverse relationship between grain size and yield strength, as demonstrated by the Hall-Petch equation. However, when there is a large direction change in the orientation of the two adjacent grains, the dislocation may not necessarily move from one grain to the other but instead create a new source of dislocation in the adjacent grain. The theory remains the same that more grain boundaries create more opposition to dislocation movement and in turn strengthens the material.

Obviously, there is a limit to this mode of strengthening, as infinitely strong materials do not exist. Grain sizes can range from about 100 μm (0.0039 in) (large grains) to 1 μm (3.9×10^{-5} in) (small grains). Lower than this, the size of dislocations begins to approach the size of the grains. At a grain size of about 10 nm (3.9×10^{-7} in), only one or two dislocations can fit inside of a grain. This scheme prohibits dislocation pile-up and never results in grain boundary diffusion. The lattice resolves the applied stress by grain boundary sliding, resulting in a *decrease* in the material's yield strength.

To understand the mechanism of grain boundary strengthening one must understand the nature of dislocation-dislocation interactions. Dislocations create a stress field around them given by:

$$\sigma \propto Gbln(\frac{r}{r_0}),$$

where G is the material's shear modulus, and b is the Burgers vector. If the dislocations are in the right alignment with respect to each other, the local stress fields they create will repel each other. This helps dislocation movement along grains and across grain boundaries. Hence, the more dislocations are present in a grain, the greater the stress field felt by a dislocation near a grain boundary:

$$\tau_{felt} = \tau_{applied} + n_{dislocation}\tau_{dislocation}$$

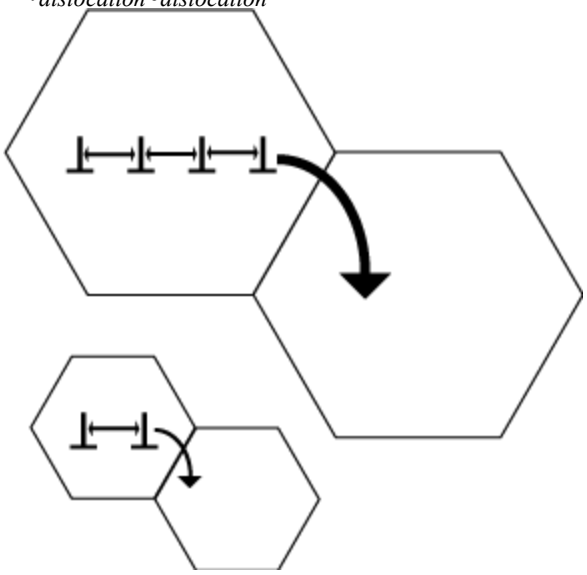

This is a schematic roughly illustrating the concept of dislocation pile up and how it affects the strength of the material. A material with larger grain size is able to have more dislocation to pile up leading to a bigger driving force for dislocations to move from one grain to another. Thus you will have to apply less force to move a dislocation from a larger than from a smaller grain, leading materials with smaller grains to exhibit higher yield stress.

Subgrain strengthening

A subgrain is a part of the grain that is only slightly disoriented from other parts of the grain. Current research is being done to see the effect of subgrain strengthening in materials. Depending on the processing of the material, subgrains can form within the grains of the material. For example, when Fe-based material is ball-milled for long periods of time (e.g. 100+ hours), subgrains of 60-90 nm are formed. It has been shown that the higher the density of the subgrains, the higher the yield stress of the material due to the increased subgrain boundary. The strength of the metal was found to vary reciprocally with the size of the subgrain, which is analogous to the Hall-Petch equation. The subgrain boundary strengthening also has a breakdown point of around a subgrain size of 0.1 nm, which is the size where any subgrains smaller than that size would decrease yield strength. .

Hall-Petch relationship

Hall-Petch constants

Material	σ_o [MPa]	k [MPa $m^{1/2}$]
Copper	25	0.11
Titanium	80	0.40
Mild steel	70	0.74
Ni_3Al	300	1.70

There is an inverse relationship between delta yield strength and grain size to some power, *x*.

$$\Delta\tau \propto \frac{k}{d^x}$$

where *k* is the strengthening coefficient and both *k* and *x* are material specific. The smaller the grain size, the smaller the repulsion stress felt by a grain boundary dislocation and the higher the applied stress needed to propagate dislocations through the material.

The relation between yield stress and grain size is described mathematically by the Hall-Petch equation:

$$\sigma_y = \sigma_0 + \frac{k_y}{\sqrt{d}}$$

where σ_y is the yield stress, σ_o is a materials constant for the starting stress for dislocation movement (or the resistance of the lattice to dislocation motion), k_y is the strengthening coefficient (a constant unique to each material), and *d* is the average grain diameter.

Theoretically, a material could be made infinitely strong if the grains are made infinitely small. This is impossible though, because the lower limit of grain size is a single unit cell of the material. Even then, if the grains of a material are the size of a single unit cell, then the material is in fact amorphous, not crystalline, since there is no long range order, and dislocations can not be defined in an amorphous material. It has been observed experimentally that the microstructure with the highest yield strength is a grain size of about 10 nm (3.9×10^{-7} in), because grains smaller than this undergo another yielding mechanism, grain boundary sliding. Producing engineering materials with this ideal grain size is difficult because only thin films can be reliably produced with grains of this size.

History

In the early 1950s two groundbreaking series of papers were written independently on the relationship between grain boundaries and strength.

In 1951, while at the University of Sheffield, E.O. Hall wrote three papers which appeared in volume 64 of the Proceedings of the Physical Society. In his third paper, Hall showed that the length of slip bands or crack lengths correspond to grain sizes and thus a relationship could be established between the two. Hall concentrated on the yielding properties of mild steels.

Based on his experimental work carried out in 1946–1949, N.J. Petch of the University of Leeds, England published a paper in 1953 independent from Hall's. Petch's paper concentrated more on brittle fracture. By measuring the variation in cleavage strength with respect to ferritic grain size at very low temperatures, Petch found a relationship exact to that of Hall's. Thus this important relationship is named after both Hall and Petch.

Reverse or inverse Hall-Petch relation

The Hall-Petch relation predicts that as the grain size decreases the yield strength increases. The Hall-Petch relation was experimentally found to be an effective model for materials with grain sizes ranging from 1 millimeter to 1 micrometre. Consequently it was believed that if average grain size could be decreased even further to the nanometer length scale the yield strength would increase as well. However, experiments on many nanocrystalline materials demonstrated that if the grains reached a small enough size, the critical grain size which is typically less than 100 nm (3.9×10^{-6} in), the yield strength would either remain constant or decrease with decreasing grains size. This phenomenon has been termed the reverse or inverse Hall-Petch Relation. A number of different mechanisms have been proposed for this relation. As suggested by Carlton et al. they fall into four categories: (1) Dislocation based (2) Diffusion based (3) Grain boundary shearing based (4) Two phase based.

Other explanations that have been proposed to rationalize the apparent softening of metals with nanosized grains include poor sample quality and the suppression of dislocation pileups.

Many of the early measurements of a reverse Hall-Petch effect were likely the result of unrecognized pores in samples. The presence of voids in nanocrystalline metals would undoubtedly lead to their having weaker mechanical properties.

The pileup of dislocations at grain boundaries is a hallmark mechanism of the Hall-Petch relationship. Once grain sizes drop below the equilibrium distance between dislocations, though, this relationship should no longer be valid. Nevertheless, it is not entirely clear what exactly the dependency of yield stress should be on grain sizes below this point.

Grain refinement

Grain refinement, also known as *inoculation*, is the set of techniques used to implement grain boundary strengthening in metallurgy. The specific techniques and corresponding mechanisms will vary based on what materials are being considered.

One method for controlling grain size in aluminum alloys is by introducing particles to serve as nucleants, such as Al-5%Ti. Grains will grow via heterogeneous nucleation; that is, for a given degree of undercooling beneath the melting temperature, aluminum particles in the melt will nucleate on the surface of the added particles. Grains will grow in the form of dendrites growing radially away from the surface of the nucleant. Solute particles can then be added (called grain refiners) which limit the growth of dendrites, leading to grain refinement. TiB2 is a common grain refiner for Al alloys; however, novel refiners such as Al3Sc have been suggested.

One common technique is to induce a very small fraction of the melt to solidify at a much higher temperature than the rest; this will generate seed crystals that act as a template when the rest of the material falls to its (lower) melting temperature and begins to solidify. Since a huge number of minuscule seed crystals are present, a nearly equal number of crystallites result, and the size of any one grain is limited.

Typical inoculants for various casting alloys

Metal	Inoculant
Cast iron	FeSi, SiCa, graphite
Mg alloys	Zr, C
Cu alloys	Fe, Co, Zr
Al-Si alloys	P, Ti, B
Pb alloys	As, Te
Zn alloys	Ti
Ti alloys	Al-Ti intermetallics

Chapter 8

Work Hardening

Work hardening, also known as **strain hardening** or **cold working**, is the strengthening of a metal by plastic deformation. This strengthening occurs because of dislocation movements within the crystal structure of the material. Any material with a reasonably high melting point such as metals and alloys can be strengthened in this fashion. Alloys not amenable to heat treatment, including low-carbon steel, are often work-hardened. Some materials cannot be work-hardened at normal ambient temperatures, such as indium, however others can only be strengthened via work hardening, such as pure copper and aluminum.

Work hardening may be desirable or undesirable depending on the context. An example of undesirable work hardening is during machining when early passes of a cutter inadvertently work-harden the workpiece surface, causing damage to the cutter during the later passes. An example of desirable work hardening is that which occurs in metalworking processes that intentionally induce plastic deformation to exact a shape change. These processes are known as **cold working** or **cold forming** processes. They are characterized by shaping the workpiece at a temperature below its recrystallization temperature, usually at the ambient temperature. Cold forming techniques are usually classified into four major groups: squeezing, bending, drawing, and shearing.

History

Copper was the first metal in common use for tools and containers since it is one of the few metals available in non-oxidized form, not requiring the smelting of an ore. Copper is easily softened by heating and cooling (it does not harden by quenching, as in cool water). In this annealed state it may then be hammered, stretched and otherwise formed, progressing toward the desired final shape, but becoming harder and less ductile as work progresses. If work continues beyond a certain hardness the metal will tend to fracture when worked and so it may be re-annealed periodically as the shape progresses. Annealing is stopped when the workpiece is near its final desired shape, and so the final

product will have a desired stiffness and hardness. The technique of repoussé exploits these properties of copper, enabling the construction of durable jewelry articles and sculptures (including the Statue of Liberty).

For metal objects designed to flex, such as springs, specialized alloys are usually employed in order to avoid work hardening (a result of plastic deformation) and metal fatigue, with specific heat treatments required to obtain the necessary characteristics.

Devices made from aluminum and its alloys, such as aircraft, must be carefully designed to minimize or evenly distribute flexure, which can lead to work hardening and in turn stress cracking, possibly causing catastrophic failure. For this reason modern aluminum aircraft will have an imposed working lifetime (dependent upon the type of loads encountered), after which the aircraft must be retired.

Theory

Before work hardening, the lattice of the material exhibits a regular, defect-free (no dislocations) pattern. The defect-free lattice can be created or restored at any time by annealing. As the material is work hardened it becomes increasingly saturated with new dislocations, and more dislocations are prevented from nucleating (a resistance to dislocation-formation develops). This resistance to dislocation-formation manifests itself as a resistance to plastic deformation; hence, the observed strengthening.

In metallic crystals, irreversible deformation is usually carried out on a microscopic scale by defects called dislocations, which are created by fluctuations in local stress fields within the material culminating in a lattice rearrangement as the dislocations propagate through the lattice. At normal temperatures the dislocations are not annihilated by annealing. Instead, the dislocations accumulate, interact with one another, and serve as pinning points or obstacles that significantly impede their motion. This leads to an increase in the yield strength of the material and a subsequent decrease in ductility.

Such deformation increases the concentration of dislocations which may subsequently form low-angle grain boundaries surrounding sub-grains. Cold working generally results in a higher yield strength as a result of the increased number of dislocations and the Hall-Petch effect of the sub-grains, and a decrease in ductility. The effects of cold working may be reversed by annealing the material at high temperatures where recovery and recrystallization reduce the dislocation density.

A material's work hardenability can be predicted by analyzing a stress-strain curve, or studied in context by performing hardness tests before and after a process.

Elastic and plastic deformation

Work hardening is a consequence of plastic deformation, a permanent change in shape. This is distinct from elastic deformation, which is reversible. Most materials do not exhibit only one or the other, but rather a combination of the two. The following

discussion mostly applies to metals, especially steels, which are well studied. Work hardening occurs most notably for ductile materials such as metals. Ductility is the ability of a material to undergo large plastic deformations before fracture (for example, bending a steel rod until it finally breaks).

The tensile test is widely used to study deformation mechanisms. This is because under compression, most materials will experience trivial (lattice mismatch) and non-trivial (buckling) events before plastic deformation or fracture occur. Hence the intermediate processes that occur to the material under uniaxial compression before the incidence of plastic deformation make the compressive test fraught with difficulties.

A material generally deforms elastically if it is under the influence of small forces, allowing the material to readily return to its original shape when the deforming force is removed. This phenomenon is called *elastic deformation*. This behavior in materials is described by Hooke's Law. Materials behave elastically until the deforming force increases beyond the elastic limit, also known as the yield stress. At this point, the material is rendered permanently deformed and fails to return to its original shape when the force is removed. This phenomenon is called *plastic deformation*. For example, if one stretches a coil spring up to a certain point, it will return to its original shape, but once it is stretched beyond the elastic limit, it will remain deformed and won't return to its original state.

Elastic deformation stretches atomic bonds in the material away from their equilibrium radius of separation of a bond, without applying enough energy to break the inter-atomic bonds. Plastic deformation, on the other hand, breaks inter-atomic bonds, and involves the rearrangement of atoms in a solid material.

Dislocations and lattice strain fields

In materials science parlance, dislocations are defined as line defects in a material's crystal structure. They are surrounded by relatively strained (and weaker) bonds than the bonds between the constituents of the regular crystal lattice. This explains why these bonds break first during plastic deformation. Like any thermodynamic system, the crystals tend to lower their energy through bond formation between constituents of the crystal. Thus the dislocations interact with one another and the atoms of the crystal. This results in a lower but energetically favorable energy conformation of the crystal. Dislocations are a "negative-entity" in that they do not exist: they are merely vacancies in the host medium which does exist. As such, the material itself does not move much. To a much greater extent visible "motion" is movement in a bonding pattern of largely stationary atoms.

The strained bonds around a dislocation are characterized by lattice strain fields. For example, there are compressively strained bonds directly next to an edge dislocation and tensilely strained bonds beyond the end of an edge dislocation. These form compressive strain fields and tensile strain fields, respectively. Strain fields are analogous to electric

fields in certain ways. Additionally, the strain fields of dislocations, obey the laws of attraction and repulsion.

The visible (macroscopic) results of plastic deformation are the result of microscopic dislocation motion. For example, the stretching of a steel rod in a tensile tester is accommodated through dislocation motion on the atomic scale.

Increase of dislocations and work hardening

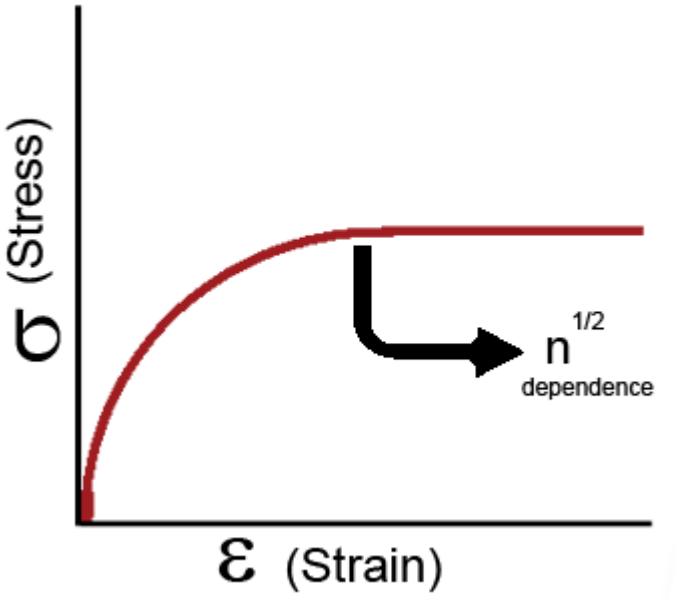

Figure 1: The yield stress of an ordered material has a half-root dependency on the number of dislocations present.

Increase in the number of dislocations is a quantification of work hardening. Plastic deformation occurs as a consequence of work being done on a material; energy is added to the material. In addition, the energy is almost always applied fast enough and in large enough magnitude to not only move existing dislocations, but also to *produce* a great number of new dislocations by jarring or working the material sufficiently enough. New dislocations are generated by Frank-Read source.

Yield strength is increased in a cold-worked material. Using lattice strain fields, it can be shown that an environment filled with dislocations will hinder the movement of any one dislocation. Because dislocation motion is hindered, plastic deformation cannot occur at normal stresses. Upon application of stresses just beyond the yield strength of the non-cold-worked material, a cold-worked material will continue to deform using the only mechanism available: elastic deformation. The regular scheme of stretching or compressing of electrical bonds (without dislocation motion) continues to occur, and the

modulus of elasticity is unchanged. Eventually the stress is great enough to overcome the strain-field interactions and plastic deformation resumes.

However, ductility of a work-hardened material is decreased. Ductility is the extent to which a material can undergo plastic deformation, that is, it is how far a material can be plastically deformed before fracture. A cold-worked material is, in effect, a normal material that has already been extended through part of its allowed plastic deformation. If dislocation motion and plastic deformation have been hindered enough by dislocation accumulation, and stretching of electronic bonds and elastic deformation have reached their limit, a third mode of deformation occurs: fracture.

Quantification of work hardening

The stress, τ, of dislocation is dependent on the shear modulus, G, the lattice constant, b, and the dislocation density, $\rho_{\perp}$:

$$\tau = \tau_0 + G\alpha b\rho_{\perp}^{1/2}$$

where τ_0 is the intrinsic strength of the material with low dislocation density and α is a correction factor specific to the material.

As shown in Figure 1 and the equation above, work hardening has a half root dependency on the number of dislocations. The material exhibits high strength if there are either high levels of dislocations (greater than 10^{14} dislocations per m^2) or no dislocations. A moderate number of dislocations (between 10^7 and 10^9 dislocations per m^2) typically results in low strength.

Example

For an extreme example, in a tensile test a bar of steel is strained to just before the distance at which it usually fractures. The load is released smoothly and the material relieves some of its strain by decreasing in length. The decrease in length is called the elastic recovery, and the end result is a work-hardened steel bar. The fraction of length recovered (length recovered/original length) is equal to the yield-stress divided by the modulus of elasticity. (Here we discuss true stress in order to account for the drastic decrease in diameter in this tensile test.) The length recovered after removing a load from a material just before it breaks is equal to the length recovered after removing a load just before it enters plastic deformation.

The work-hardened steel bar has a large enough number of dislocations that the strain field interaction prevents all plastic deformation. Subsequent deformation requires a stress that varies linearly with the strain observed, the slope of the graph of stress vs. strain is the modulus of elasticity, as usual.

The work-hardened steel bar fractures when the applied stress exceeds the usual fracture stress and the strain exceeds usual fracture strain. This may be considered to be the elastic

limit and the yield stress is now equal to the fracture toughness, which is of course, much higher than a non-work-hardened-steel yield stress.

The amount of plastic deformation possible is zero, which is obviously less than the amount of plastic deformation possible for a non-work-hardened material. Thus, the ductility of the cold-worked bar is reduced.

Substantial and prolonged cavitation can also produce strain hardening.

Additionally, jewelers will construct structurally sound rings and other wearable objects (especially those worn on the hands) that require much more durability (than earrings for example) by utilizing a material's ability to be work hardened. While casting rings is done for a number of economical reasons (saving a great deal of time and cost of labor), a master jeweler may utilize the ability of a material to be work hardened and apply some combination of cold forming techniques during the production of a piece.

Empirical relations

There are two common mathematical descriptions of the work hardening phenomenon. Hollomon's equation is a power law relationship between the stress and the amount of plastic strain:

$$\sigma = K\epsilon_p^n$$

where σ is the stress, K is the strength index, ε_p is the plastic strain and n is the strain hardening index. Ludwik's equation is similar but includes the yield stress:

$$\sigma = \sigma_y + K\epsilon_p^n$$

If a material has been subjected to prior deformation (at low temperature) then the yield stress will be increased by a factor depending on the amount of prior plastic strain ε_0:

$$\sigma = \sigma_y + K(\epsilon_0 + \epsilon_p)^n$$

The constant K is structure dependent and is influenced by processing while n is a material property normally lying in the range 0.2–0.5. The strain hardening index can be described by:

$$n = \frac{d\log(\sigma)}{d\log(\epsilon)} = \frac{\epsilon}{\sigma}\frac{d\sigma}{d\epsilon}$$

This equation can be evaluated from the slope of a log(σ) - log(ε) plot. Rearranging allows a determination of the rate of strain hardening at a given stress and strain:

$$\frac{d\sigma}{d\epsilon} = n\frac{\sigma}{\epsilon}$$

Processes

The following is a list of cold forming processes:

- Squeezing
  - Rolling
  - Swaging
  - Extrusion
  - Forging
  - Sizing
  - Riveting
  - Staking
  - Coining
  - Peening
  - Burnishing
  - Hubbing
  - Thread rolling
- Bending
  - Angle bending
  - Roll bending
  - Draw and compression
  - Roll forming
  - Seaming
  - Flanging
  - Straightening
- Shearing
  - Slitting
  - Blanking
  - Piercing
  - Lancing
  - Perforating
  - Notching
  - Nibbling
  - Shaving
  - Trimming
  - Cutoff
  - Dinking
- Drawing
  - Tube drawing
  - Wire drawing
  - Spinning

- Embossing
- Stretch forming
- Sheet metal drawing
- Ironing
- Superplastic forming

Techniques have been designed to maintain the general shape of the workpiece during work hardening, including shot peening and equal channel angular extrusion.

Advantages and disadvantages

Advantages:

- No heating required
- Better surface finish
- Superior dimensional control
- Better reproducibility and interchangeability
- Directional properties can be imparted into the metal
- Contamination problems are minimized

The increase in strength due to strain hardening is comparable to that of heat treating. Therefore, it is sometimes more economical to cold work a less costly and weaker metal than to hot work a more expensive metal that can be heat treated, especially if precision or a fine surface finish is required as well. The cold working process also reduces waste as compared to machining, or even eliminates with near net shape methods. The material savings becomes even more significant at larger volumes, and even more so when using expensive materials, such as copper. The saving on raw material as a result of cold forming can be very significant, as is saving machining time. Production cycle times when cold working are very short. On multi-station machinery, production cycle times are even less. This can be very advantageous for large production runs.

During cold working the part undergoes work hardening and the microstructure deforms to follow the contours of the part surface. Unlike hot working, the inclusions and grains distort to follow the contour of the surface, resulting in anisotropic engineering properties.

Disadvantages:

- Greater forces are required
- Heavier and more powerful equipment and stronger tooling are required
- Metal is less ductile
- Metal surfaces must be clean and scale-free
- Intermediate anneals may be required to compensate for loss of ductility that accompanies strain hardening
- The imparted directional properties may be detrimental
- Undesirable residual stress may be produced

Due to the large capital costs required to set up a cold working process the process is usually only suitable for large volume productions.

Intermediate annealings may be required to reach the required ductility to continue cold working a workpiece, otherwise it may fracture if the ultimate tensile strength is exceeded. An anneal may also be used to obtain the proper engineering properties required in the final workpiece. Also, the distorted grain structure that gives the workpiece its superior strength can lead to residual stresses.

Cold worked items suffer from a phenomenon known as *springback*, or *elastic springback*. After the deforming force is removed from the workpiece, the workpiece springs back slightly. The amount a material springs back is equal to Young's modulus for the material from the final stress.

Chapter 9

Solid Solution Strengthening

Solid solution strengthening is a type of alloying that can be used to improve the strength of a pure metal. The technique works by adding atoms of one element (the alloying element) to the crystalline lattice of another element (the base metal). The alloying element diffuses into the matrix, forming a solid solution. In most binary systems, when alloyed above a certain concentration, a second phase will form. When this increases the strength of the material, the process is known as precipitation strengthening, but this is not always the case.

Types

Depending on the size of the alloying element, a substitutional solid solution or an interstitial solid solution can form. In both cases, the overall crystal structure is essentially unchanged.

Substitutional solid solution strengthening occurs when the solute atom is large enough that it can replace solvent atoms in their lattice positions. According to the Hume-Rothery rules, solvent and solute atoms must differ in atomic size by less than 15% in order to form this type of solution. Because both elements exist in the same crystalline lattice, both elements in their pure form must be of the same crystal structure. Examples of substitutional solid solutions include the Cu-Ni and the Ag-Au FCC binary systems, and the Mo-W BCC binary system.

When the solute atom is much smaller than the solvent atoms, an interstitial solid solution forms. This typically occurs when the solute atoms are less than half as small as the solvent atoms. The smaller solute atom essentially "crowds" into the spacings within the lattice structure, causing defects in the material. Elements commonly used to form interstitial solid solutions include H, N, C, and O. Carbon in iron (steel) is one example of interstitial diffusion.

Mechanism

The strength of a material is dependent on how easily dislocations in its crystal lattice can be propagated. These dislocations create stress fields within the material depending on their character. When solute atoms are introduced, local stress fields are formed that interact with those of the dislocations, impeding their motion and causing an increase in the yield stress of the material, which means an increase in strength of the material. This gain is a result of both lattice distortion and the modulus effect.

When solute and solvent atoms differ in size, local stress fields are created (if solute atom size is larger than solvent atom size, this field is compressive, and similarly, when solute atoms are smaller than solvent atoms, this field is tensile). Depending on their relative locations, solute atoms will either attract or repel dislocations in their vicinity. This is known as the size effect. This allows the solute atoms to relieve either tensile or compressive strain in the lattice, which in turn puts the dislocation in a lower energy state. In substitutional solid solutions, these stress fields are spherically symmetric, meaning they have no shear stress component. As such, substitutional solute atoms do not interact with the shear stress fields characteristic of screw dislocations. Conversely, in interstitial solid solutions, solute atoms cause a tetragonal distortion, generating a shear field that can interact with both edge, screw, and mixed dislocations. The attraction or repulsion of the dislocation centers to the solute particles increase the stress it takes to propagate the dislocation in any other direction. Increasing the applied stress to move the dislocation increases the yield strength of the material.

The energy density of a dislocation is dependent on its Burgers vector as well as the modulus of the local atoms. When the modulus of solute atoms differs from that of the host element, the local energy around the dislocation is changed, increasing the amount of force necessary to move past this energy well. This is known as the modulus effect. Meanwhile, in the specific case of a lattice distortion, the difference in lattice parameter leads to a high stress field around that solute atom that impedes dislocation movement.

Surface carburizing, or case hardening, is one example of solid solution strengthening in which the density of solute carbon atoms is increased close to the surface of the steel, resulting in a gradient of carbon atoms throughout the material. This provides superior mechanical properties to the surface of the steel.

Governing equations

Solid solution strengthening increases yield strength of the material by increasing the stress τ to move dislocations:

$$\Delta\tau = Gb\epsilon^{\frac{3}{2}}\sqrt{c}$$

where c is the concentration of the solute atoms, G is the shear modulus, b is the magnitude of the Burger's vector, and ε is the lattice strain due to the solute. This is

composed of two terms, one describing lattice distortion and the other local modulus change.

$\varepsilon = | \varepsilon_a - \beta\varepsilon_G |$ Here, ε_a is the lattice distortion term, β a constant dependent on the solute atoms and ε_G the term that captures the local modulus change.

The lattice distortion term can be described as:

$\epsilon_a = \frac{\Delta a}{a \Delta c}$, where *a* is the lattice parameter of the material.

Meanwhile, the local modulus change is captured in the following expression:

$\epsilon_G = \frac{\Delta G}{G \Delta c}$, where *G* is shear modulus of the solute material,

Implications

In order to achieve noticeable material strengthening via solute solution strengthening one should alloy with solutes of higher shear modulus, hence increasing the local shear modulus in the material. In addition, one should alloy with elements of different equilibrium lattice constants. The greater the different in lattice parameter, the higher the local stress fields introduced by alloying. Alloying with elements of higher shear modulus or of very different lattice parameters will increase the stiffness and introduce local stress fields respectively. In either case, the dislocation propagation will be hindered at these sites, impeding plasticity and increasing yield strength proportionally with solute concentration.

Solid solution strengthening depends on:
- Concentration of solute atoms
- Shear modulus of solute atoms
- Size of solute atoms
- Valency of solute atoms (for ionic materials)

Nevertheless, one should not add so much solute as to precipitate a new phase. This occurs if the concentration of the solute reaches a high critical point given by the binary system phase diagram. This critical concentration therefore puts a limit to the amount of solid solution strengthening a material can have, as the material cannot be infinitely strengthened.

Chapter 10

Precipitation Hardening

Precipitation hardening, also called **age hardening**, is a heat treatment technique used to increase the yield strength of malleable materials, including most structural alloys of aluminium, magnesium, nickel and titanium, and some stainless steels. It relies on changes in solid solubility with temperature to produce fine particles of an impurity phase, which impede the movement of dislocations, or defects in a crystal's lattice. Since dislocations are often the dominant carriers of plasticity, this serves to harden the material. The impurities play the same role as the particle substances in particle-reinforced composite materials. Just as the formation of ice in air can produce clouds, snow, or hail, depending upon the thermal history of a given portion of the atmosphere, precipitation in solids can produce many different sizes of particles, which have radically different properties. Unlike ordinary tempering, alloys must be kept at elevated temperature for hours to allow precipitation to take place. This time delay is called **aging**.

Note that two different heat treatments involving precipitates can alter the strength of a material: solution heat treating and precipitation heat treating. Solid solution strengthening involves formation of a single-phase solid solution via quenching and leaves a material softer. Precipitation heat treating involves the addition of impurity particles to increase a material's strength.

Kinetics versus thermodynamics

This technique exploits the phenomenon of supersaturation, and involves careful balancing of the driving force for precipitation and the thermal activation energy available for both desirable and undesirable processes.

Nucleation occurs at a relatively high temperature (often just below the solubility limit) so that the kinetic barrier of surface energy can be more easily overcome and the maximum number of precipitate particles can form. These particles are then allowed to grow at lower temperature in a process called *aging*. This is carried out under conditions of low solubility so that thermodynamics drive a greater total volume of precipitate formation.

Diffusion's exponential dependence upon temperature makes precipitation strengthening, like all heat treatments, a fairly delicate process. Too little diffusion (*under aging*), and the particles will be too small to impede dislocations effectively; too much (*over aging*), and they will be too large and dispersed to interact with the majority of dislocations.

Alloy design

Precipitation strengthening is possible if the line of solid solubility slopes strongly toward the center of a phase diagram. While a large volume of precipitate particles is desirable, a small enough amount of the alloying element should be added that it remains easily soluble at some reasonable annealing temperature.

Elements used for precipitation strengthening in typical aluminum and titanium alloys, make up about 10% of their composition. While binary alloys are more easily understood as an academic exercise, commercial alloys often use three components for precipitation strengthening, in compositions such as Al(Mg, Cu) and Ti(Al, V). A large number of other constituents may be unintentional, but benign, or may be added for other purposes such as grain refinement or corrosion resistance. In some cases, such as many aluminum alloys, an increase in strength is achieved at the expense of corrosion resistance.

The addition of large amounts of nickel and chromium needed for corrosion resistance in stainless steels means that traditional hardening and tempering methods are not effective. However, precipitates of chromium, copper or other elements can strengthen the steel by similar amounts in comparison to hardening and tempering. The strength can be tailored by adjusting the annealing process, with lower initial temperatures resulting in higher strengths. The lower initial temperature increase driving force of nucleation. More driving force means more nucleation sites, and more sites, means more places for dislocations to be disrupted while the finished part is in use.

Many alloy systems allow the aging temperature to be adjusted. For instance, some aluminium alloys used to make rivets for aircraft construction are kept in dry ice from their initial heat treatment until they are installed in the structure. After this type of rivet is deformed into its final shape, aging occurs at room temperature and increases its strength, locking the structure together. Higher aging temperatures would risk over-aging other parts of the structure, and require expensive post-assembly heat treatment. Too high of an aging temperature promotes the precipitate to grow too readily.

Theory

The primary species of precipitation strengthening are second phase particles. These particles impede the movement of dislocations throughout the lattice. You can determine whether or not second phase particles will precipitate into solution from the solidus line on the phase diagram for the particles. Physically, this strengthening effect can be attributed both to size and modulus effects, and to interfacial or surface energy.

The presence of second phase particles often causes lattice distortions. These lattice distortions result when the precipitate particles differ in size from the host atoms. Smaller precipitate particles in a host lattice leads to a tensile stress, whereas larger precipitate particles leads to a compressive stress. Dislocation defects also create a stress field. Above the dislocation there is a compressive stress and below there is a tensile stress. Consequently, there is a negative interaction energy between a dislocation and a precipitate that each respectively cause a compressive and a tensile stress or vice versa. In other words, the dislocation will be attracted to the precipitate. In addition, there is a positive interaction energy between a dislocation and a precipitate that have the same type of stress field. This means that the dislocation will be repulsed by the precipitate.

Precipitate particles also serve by locally changing the stiffness of a material. Dislocations are repulsed by regions of higher stiffness. Conversely, if the precipitate causes the material to be locally more compliant, then the dislocation will be attracted to that region.

Furthermore, a dislocation may cut through a precipitate particle. This interaction causes an increase in the surface area of the particle. The area created is

$$A = 2rb\pi$$

where, r is the radius of the particle and b is the magnitude of the burgers vector. The resulting increase in surface energy is

$$E = 2rb\pi\gamma_s$$

where γ_s is the surface energy. The dislocation can also bow around a precipitate particle.

Governing Equations

There are two equations to describe the two mechanisms for precipitation hardening:

Dislocations cutting through particles:

$$\tau = \frac{r\gamma\pi}{bL}$$

where τ is material strength, *r* is the second phase particle radius, γ is the surface energy, *b* is the magnitude of the Burgers vector, and *L* is the spacing between pinning points. This governing equation shows that the strength is proportional to *r*, the radius of the precipitate particles. This means that it is easier for dislocations to cut through a material with smaller second phase particles (small r). As the size of the second phase particles increases, the particles impede dislocation movement and it becomes increasingly difficult for the particles to cut through the material. In other words, the strength of a material increases with increasing r.

Dislocations bowing around particle:

$$\tau = \frac{Gb}{L - 2r}$$

where τ is the material strength, G is the shear modulus, b is the magnitude of the Burgers vector, L is the distance between pinning points, and r is the second phase particle radius. This governing equation shows that for dislocation bowing the strength is inversely proportional to the second phase particle radius r. Dislocation bowing is more likely to occur when there are large particles present in the material.

These governing equations show that the precipitation hardening mechanism depends on the size of the precipitate particles. At small r, cutting will dominate, while at large r, bowing will dominate.

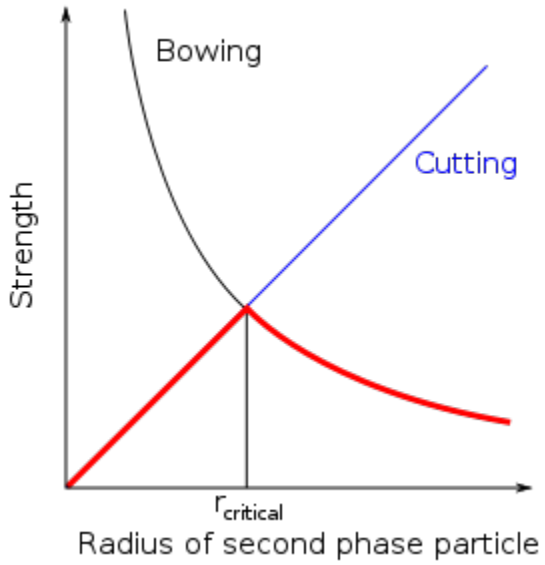

Looking at the plot of both equations, it is clear that there is a critical radius at which max strengthening occurs. This critical radius is typically 5-30 nm.

Some precipitation hardening materials

- 2000-series aluminum alloys (important examples: 2024 and 2019, also Y alloy and Hiduminium)
- 6000-series aluminum alloys (important example: 6061 for bicycle frames and aeronautical structures)
- 7000-series aluminum alloys (important examples: 7075 and 7475)
- 17-4PH stainless steel (UNS S17400)
- Maraging steel
- Inconel 718
- Alloy X-750

- René 41
- Waspaloy

Chapter 11

Von Mises Yield Criterion

The **Von Mises yield criterion** suggests that the yielding of materials begins when the second deviatoric stress invariant J_2 reaches a critical value k. For this reason, it is sometimes called the J_2-*plasticity* or J_2 flow theory. It is part of a plasticity theory that applies best to ductile materials, such as metals. Prior to yield, material response is assumed to be elastic.

In materials science and engineering the von Mises yield criterion can be also formulated in terms of the **von Mises stress** or **equivalent tensile stress**, σ_v, a scalar stress value that can be computed from the stress tensor. In this case, a material is said to start yielding when its von Mises stress reaches a critical value known as the yield strength, σ_y. The von Mises stress is used to predict yielding of materials under any loading condition from results of simple uniaxial tensile tests. The von Mises stress satisfies the property that two stress states with equal distortion energy have equal von Mises stress.

Because the von Mises yield criterion is independent of the first stress invariant, I_1, it is applicable for the analysis of plastic deformation for ductile materials such as metals, as the onset of yield for these materials does not depend on the hydrostatic component of the stress tensor.

Although formulated by Maxwell in 1865, it is generally attributed to Richard Edler von Mises (1913). Tytus Maksymilian Huber (1904), in a paper in Polish, anticipated to some extent this criterion. This criterion is also referred to as the Maxwell–Huber–Hencky–von Mises theory.

Mathematical formulation

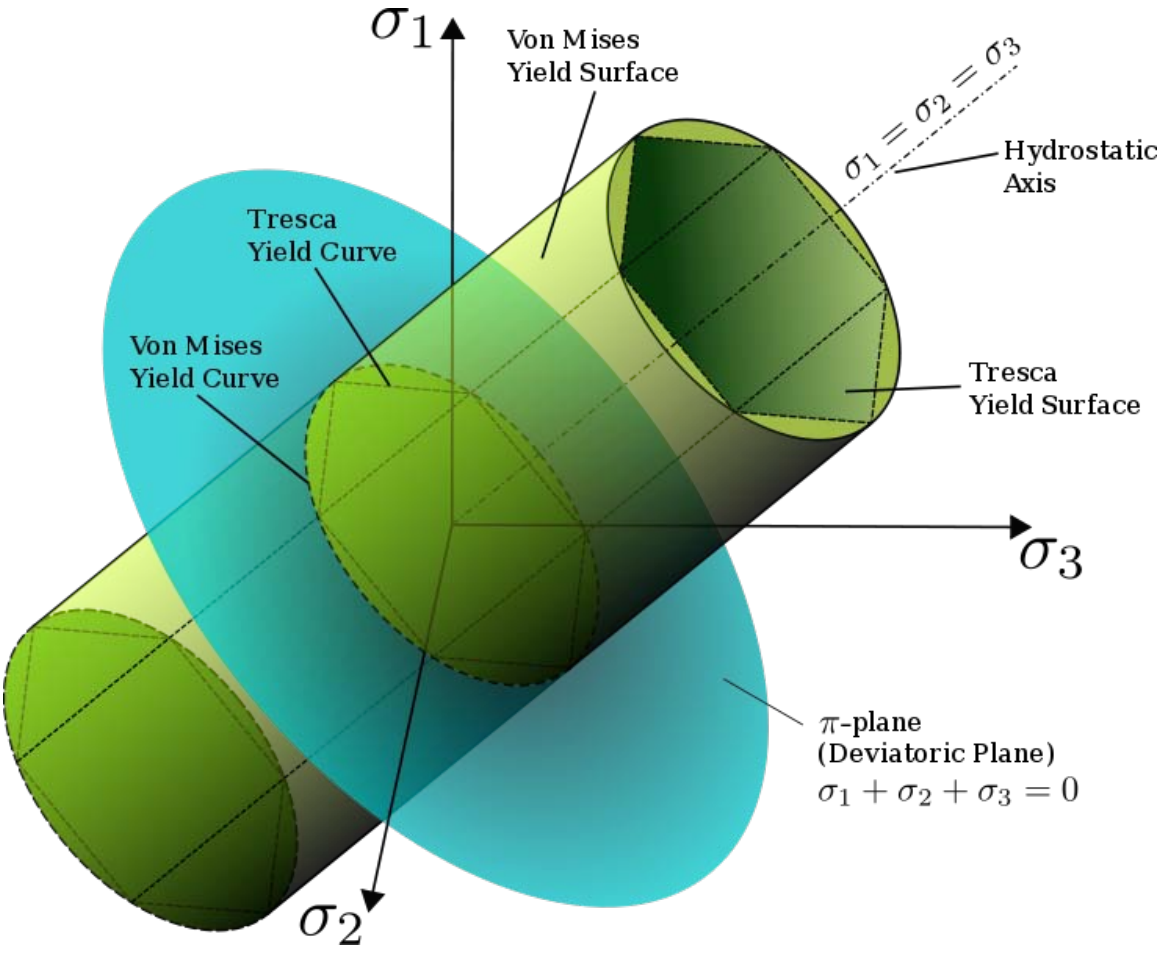

The von Mises yield surfaces in principal stress coordinates circumscribes a cylinder with radius $\sqrt{\frac{2}{3}}\sigma_y$ around the hydrostatic axis. Also shown is Tresca's hexagonal yield surface.

Mathematically the yield function for the von Mises condition is expressed as:

$$f(J_2) = \sqrt{J_2} - k = 0$$

An alternative form is:

$$f(J_2) = J_2 - k^2 = 0$$

where *k* can be shown to be the yield stress of the material in pure shear. As it will become evident later here, at the onset of yielding, the magnitude of the shear yield stress in pure shear is √3 times lower than the tensile yield stress in the case of simple tension. Thus, we have

$$k = \frac{\sigma_y}{\sqrt{3}}$$

Furthermore, if we define the von Mises stress as $\sigma_v = \sqrt{3J_2}$, the von Mises yield criterion can be expressed as:

$$\begin{aligned} f(J_2) &= \sqrt{3J_2} - \sigma_y \\ &= \sigma_v - \sigma_y = 0 \end{aligned}$$

Substituting J_2 in terms of the principal stresses into the von Mises criterion equation we have

$$(\sigma_1 - \sigma_2)^2 + (\sigma_2 - \sigma_3)^2 + (\sigma_1 - \sigma_3)^2 = 6k^2 = 2\sigma_y^2$$

or

$$(\sigma_1^2 + \sigma_2^2 + \sigma_3^2) - \sigma_1\sigma_2 - \sigma_2\sigma_3 - \sigma_1\sigma_3 = 3k^2 = \sigma_y^2$$

or as a function of the stress tensor components

$$(\sigma_{11} - \sigma_{22})^2 + (\sigma_{22} - \sigma_{33})^2 + (\sigma_{11} - \sigma_{33})^2 + 6(\sigma_{23}^2 + \sigma_{31}^2 + \sigma_{12}^2) = 6k^2 = 2\sigma_y^2$$

This equation defines the yield surface as a circular cylinder whose yield curve, or intersection with the deviatoric plane, is a circle with radius $\sqrt{2}k$, or $\sqrt{\frac{2}{3}}\sigma_y$. This implies that the yield condition is independent of hydrostatic stresses.

Von Mises criterion for different stress conditions

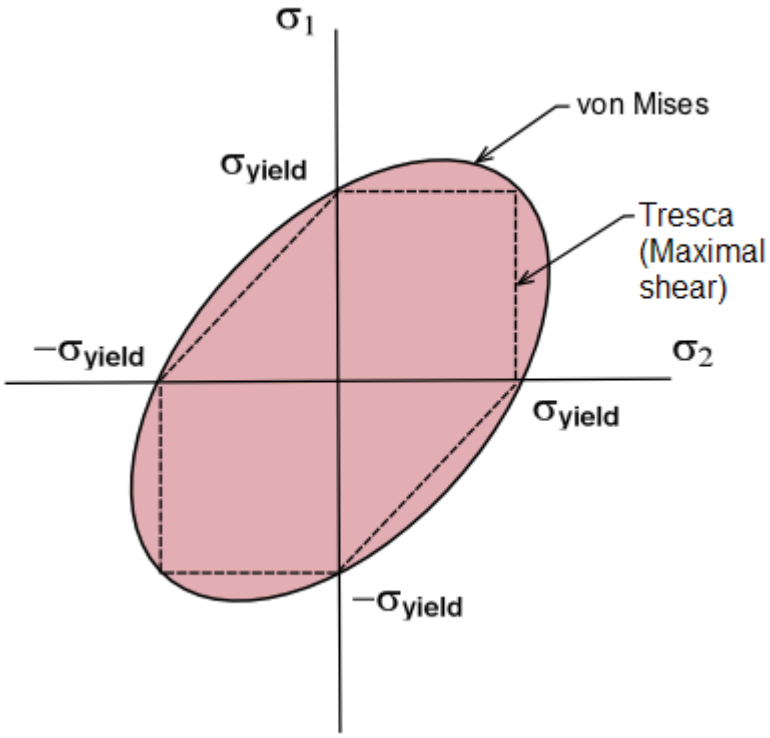

Projection of the von Mises yield criterion into the σ_1,σ_2 plane

In the case of **uniaxial stress** or **simple tension**, $\sigma_1 \neq 0$, $\sigma_3 = \sigma_2 = 0$, the von Mises criterion reduces to

$$\sigma_1 = \sigma_y.$$

Therefore, the material starts to yield, when σ_1 reaches the *yield strength* of the material σ_y, which is a characteristic material property. In practice, this parameter is indeed determined in a tensile test satisfying the uniaxial stress condition.

It is also convenient to define an **Equivalent tensile stress** or **von Mises stress**, σ_v, which is used to predict yielding of materials under **multiaxial loading conditions** using results from simple uniaxial tensile tests. Thus, we define

$$\begin{aligned}\sigma_v &= \sqrt{3J_2} \\ &= \sqrt{\frac{(\sigma_{11}-\sigma_{22})^2+(\sigma_{22}-\sigma_{33})^2+(\sigma_{11}-\sigma_{33})^2+6(\sigma_{12}^2+\sigma_{23}^2+\sigma_{31}^2)}{2}} \\ &= \sqrt{\frac{(\sigma_1-\sigma_2)^2+(\sigma_2-\sigma_3)^2+(\sigma_1-\sigma_3)^2}{2}} \\ &= \sqrt{\tfrac{3}{2}\, s_{ij}s_{ji}}\end{aligned}$$

where s_{ij} are the components of the stress deviator tensor $\boldsymbol{\sigma}^{dev}$:

$$\boldsymbol{\sigma}^{dev} = \boldsymbol{\sigma} - \frac{1}{3}(\boldsymbol{\sigma}\cdot\mathbf{I})\,\mathbf{I}$$

In this case, yielding occurs when the equivalent stress, σ_v, reaches the yield strength of the material in simple tension, σ_y. As an example, the stress state of a steel beam in compression differs from the stress state of a steel axle under torsion, even if both specimen are of the same material. In view of the stress tensor, which fully describes the stress state, this difference manifests in six degrees of freedom, because the stress tensor has six independent components. Therefore, it is difficult to tell which of the two specimens is closer to the yield point or has even reached it. However, by means of the von Mises yield criterion, which depends solely on the value of the scalar von Mises stress, i.e., one degree of freedom, this comparison is straightforward: A larger von Mises value implies that the material is closer to the yield point.

In the case of **pure shear stress**, $\sigma_{12} = \sigma_{21} \neq 0$, while all other $\sigma_{ij} = 0$, von Mises criterion becomes:

$$\sigma_{12} = k = \frac{\sigma_y}{\sqrt{3}}$$

This means that, at the onset of yielding, the magnitude of the shear stress in pure shear is $\sqrt{3}$times lower than the tensile stress in the case of simple tension. The von Mises yield criterion for pure shear stress, expressed in principal stresses, is

$$(\sigma_1-\sigma_2)^2+(\sigma_2-\sigma_3)^2+(\sigma_1-\sigma_3)^2 = 6\sigma_{12}^2$$

In the case of **plane stress**, $\sigma_3 = 0$, the von Mises criterion becomes:

$$\sigma_1^2 - \sigma_1\sigma_2 + \sigma_2^2 = 3k^2 = \sigma_y^2$$

This equation represents an ellipse in the plane $\sigma_1 - \sigma_2$, as shown in the Figure above.

Physical interpretation of the von Mises yield criterion

Hencky (1924) offered a physical interpretation of von Mises criterion suggesting that yielding begins when the elastic energy of distortion reaches a critical value. For this, the von Mises criterion is also known as the **maximum distortion strain energy criterion**. This comes from the relation between J_2 and the elastic strain energy of distortion W_D:

$$W_D = \frac{J_2}{2G} \text{ with the elastic shear modulus } G = \frac{E}{2(1+\nu)}.$$

In 1937 Arpad L. Nadai suggested that yielding begins when the octahedral shear stress reaches a critical value, i.e. the octahedral shear stress of the material at yield in simple tension. In this case, the von Mises yield criterion is also known as the **maximum octahedral shear stress criterion** in view of the direct proportionality that exist between J_2 and the octahedral shear stress, τ_{oct}, which by definition is

$$\tau_{oct} = \sqrt{\tfrac{2}{3} J_2}$$

thus we have

$$\tau_{oct} = \tfrac{\sqrt{2}}{3}\sigma_y$$

Comparison with Tresca yield criterion

Also shown in the figure is Tresca's maximum shear stress criterion (dashed line). Observe that Tresca's yield surface is circumscribed by von Mises'. Therefore, it predicts plastic yielding already for stress states that are still elastic according to the von Mises criterion. As a model for plastic material behavior, Tresca's criterion is therefore more conservative.

Chapter 12

Yield Surface

A **yield surface** is a five-dimensional surface in the six-dimensional space of stresses. The yield surface is usually convex and the state of stress of *inside* the yield surface is elastic. When the stress state lies on the surface the material is said to have reached its yield point and the material is said to have become plastic. Further deformation of the material causes the stress state to remain on the yield surface, even though the surface itself may change shape and size as the plastic deformation evolves. This is because stress states that lie outside the yield surface are non-permissible in rate-independent plasticity, though not in some models of viscoplasticity.

The yield surface is usually expressed in terms of (and visualized in) a three-dimensional principal stress space (σ_1,σ_2,σ_3), a two- or three-dimensional space spanned by stress invariants (I_1,J_2,J_3) or a version of the three-dimensional Haigh–Westergaard stress space. Thus we may write the equation of the yield surface (that is, the yield function) in the forms:

- $f(\sigma_1, \sigma_2, \sigma_3) = 0$ where σ_i are the principal stresses.
- $f(I_1, J_2, J_3) = 0$ where I_1 is the first principal invariant of the Cauchy stress and J_2,J_3 are the second and third principal invariants of the deviatoric part of the Cauchy stress.
- $f(p, q, r) = 0$ where p,q are scaled versions of I_1 and J_2 and r is a function of J_2,J_3.
- $f(\xi, \rho, \theta) = 0$ where ξ,ρ are scaled versions of I_1 and J_2, and θ is the **Lode angle**.

Invariants used to describe yield surfaces

The first principal invariant of the Cauchy stress (I_1), and the second and third principal invariants of the deviatoric part of the Cauchy stress (J_2,J_3) are defined as

$$I_1 = \mathrm{Tr}(\boldsymbol{\sigma}) = \sigma_1 + \sigma_2 + \sigma_3$$
$$J_2 = \frac{1}{2}\boldsymbol{s} : \boldsymbol{s} = \frac{1}{6}\left[(\sigma_1 - \sigma_2)^2 + (\sigma_2 - \sigma_3)^2 + (\sigma_3 - \sigma_1)^2\right]$$
$$J_3 = \det(\boldsymbol{s}) = \frac{1}{3}(\boldsymbol{s} \cdot \boldsymbol{s}) : \boldsymbol{s} = s_1 s_2 s_3$$

where $\boldsymbol{\sigma}$ is the Cauchy stress and $\sigma_1,\sigma_2,\sigma_3$ are its principal values, $\boldsymbol{s}$ is the deviatoric part of the Cauchy stress and s_1,s_2,s_3 are its principal values.

The quantities p, q, r are usually used to describe yield surfaces for cohesive frictional materials such as rocks, soils, and ceramics. These quantities are defined as

$$p = \frac{1}{3} I_1 \ : \quad q = \sqrt{3\ J_2} = \sigma_{\text{eq}} \ ; \quad r = 3 \left(\frac{J_3}{2}\right)^{1/3}$$

where σ_{eq} is the **equivalent stress**.

The quantities ξ, ρ, θ describe a cylindrical coordinate system (the **Haigh–Westergaard** coordinates) and are defined as

$$\xi = \frac{1}{\sqrt{3}} I_1 = \sqrt{3}\, p \ ; \quad \rho = \sqrt{2J_2} = \sqrt{\frac{2}{3}}\, q \ ; \quad \cos(3\theta) = \left(\frac{r}{q}\right)^3 = \frac{3\sqrt{3}}{2}\, \frac{J_3}{J_2^{3/2}}$$

The $\xi - \rho$ plane is also called the **Rendulic plane**. The angle θ is called the **Lode angle** and the relation between θ and J_2,J_3 was first given by Nayak and Zienkiewicz in 1972

The principal stresses and the Haigh–Westergaard coordinates are related by

$$\begin{bmatrix} \sigma_1 \\ \sigma_2 \\ \sigma_3 \end{bmatrix} = \frac{1}{\sqrt{3}} \begin{bmatrix} \xi \\ \xi \\ \xi \end{bmatrix} + \sqrt{\frac{2}{3}}\, \rho \begin{bmatrix} \cos\theta \\ \cos\left(\theta - \dfrac{2\pi}{3}\right) \\ \cos\left(\theta + \dfrac{2\pi}{3}\right) \end{bmatrix}$$

Examples of yield surfaces

There are several different yield surfaces known in engineering, and those most popular are listed below.

Tresca yield surface

The Tresca or *maximum shear stress* yield criterion is taken to be the work of Henri Tresca. It is also referred as the Tresca–Guest (TG) criterion. The functional form of this yield criterion is

$$f(\sigma_1, \sigma_2, \sigma_3) = 0 \ .$$

In terms of the principal stresses the Tresca criterion is expressed as

$$\max(|\sigma_1 - \sigma_2|, |\sigma_2 - \sigma_3|, |\sigma_3 - \sigma_1|) = \sigma_0$$

Figure 1 shows the Tresca–Guest yield surface in the three-dimensional space of principal stresses. It is a prism of six sides and having infinite length. This means that the material remains elastic when all three principal stresses are roughly equivalent (a hydrostatic pressure), no matter how much it is compressed or stretched. However, when one of principal stresses becomes smaller (or larger) than the others the material is subject to shearing. In such situations, if the shear stress reaches the yield limit then the material enters the plastic domain. Figure 2 shows the Tresca–Guest yield surface in two-dimensional stress space, it is a cross section of the prism along the σ_1,σ_2 plane.

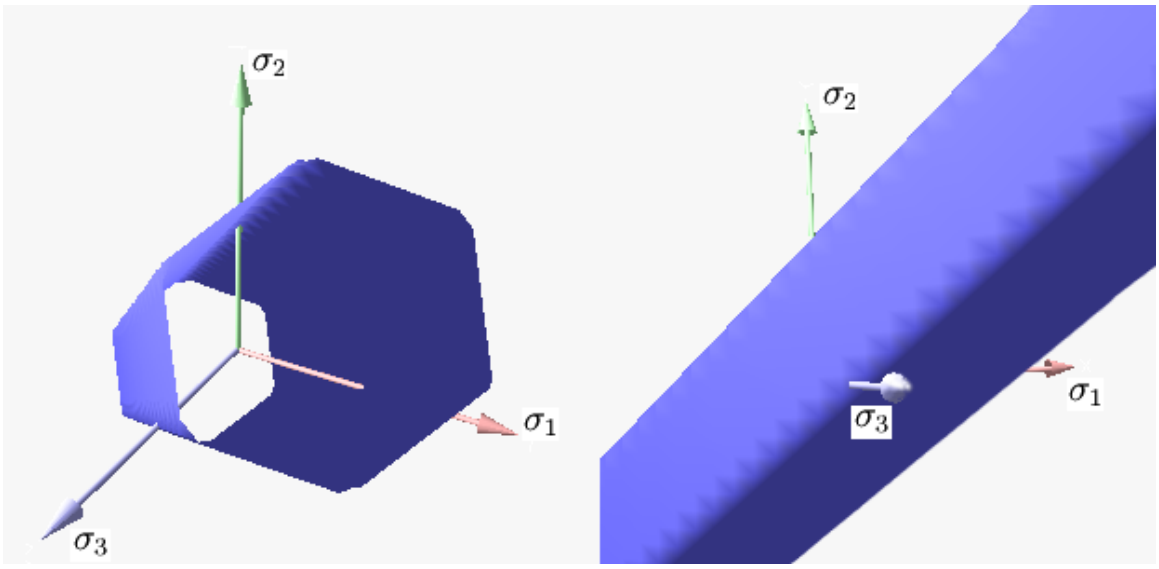

Figure 1: View of Tresca–Guest yield surface in 3D space of principal stresses

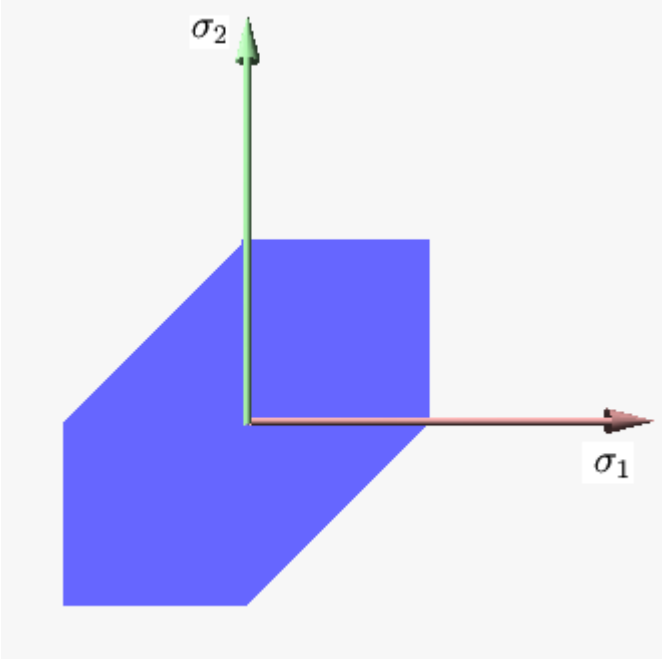

Figure 2: Tresca–Guest yield surface in 2D space (σ_1,σ_2)

Huber–von Mises yield surface

The von Mises yield criterion (also known as Prandtl–Reuss yield criterion) has the functional form

$$f(J_2) = 0 \ .$$

This yield criterion is often credited to Maximilian Huber and Richard von Mises. It is also referred to as the Huber–Mises–Hencky (HMH) criterion.

The von Mises yield criterion is expressed in the principal stresses as

$$\sqrt{3J_2} = \sigma_y \quad \text{or,} \quad (\sigma_1 - \sigma_2)^2 + (\sigma_2 - \sigma_3)^2 + (\sigma_3 - \sigma_1)^2 = 2{\sigma_y}^2$$

where σ_y is the yield stress in uniaxial tension.

Figure 3 shows the von Mises yield surface in the three-dimensional space of principal stresses. It is a circular cylinder of infinite length with its axis inclined at equal angles to the three principal stresses. Figure 4 shows the von Mises yield surface in two-dimensional space compared with Tresca–Guest criterion. A cross section of the von Mises cylinder on the plane of σ_1,σ_2 produces the elliptical shape of the yield surface.

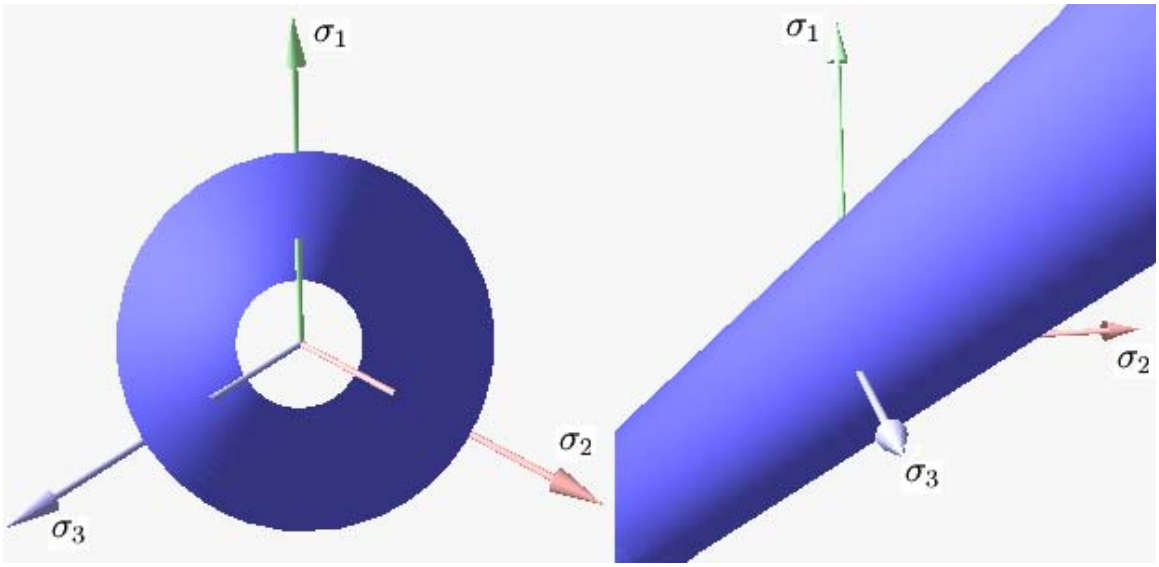

Figure 3: View of Huber–Mises–Hencky yield surface in 3D space of principal stresses

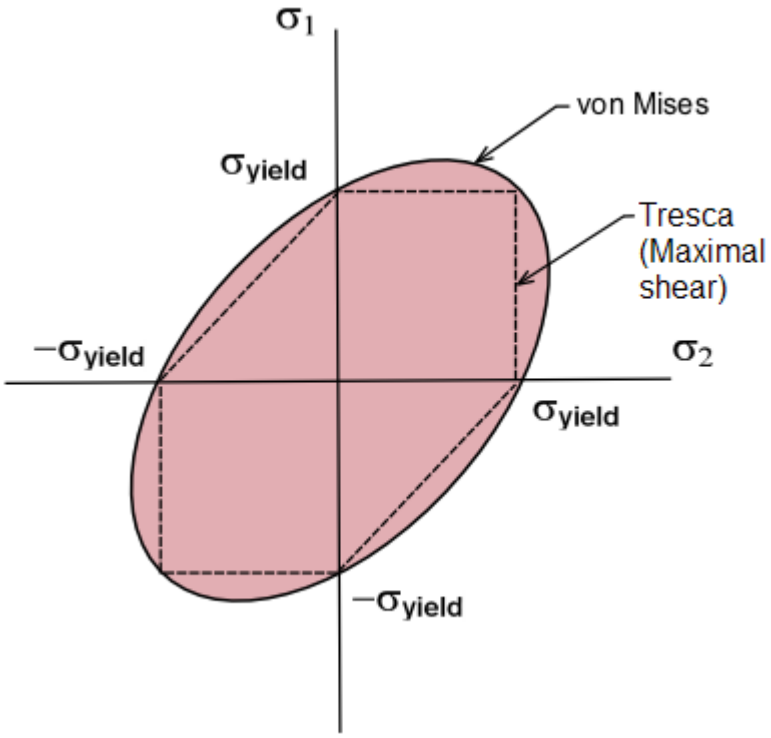

Figure 4: Comparison of Tresca–Guest and Huber–Mises–Hencky criteria in 2D space (σ_1,σ_2)

Mohr–Coulomb yield surface

The Mohr–Coulomb yield (failure) criterion is a two-parameter yield criterion which has the functional form

$f(\sigma_1,\sigma_2,\sigma_3) = 0$

This model is often used to model concrete, soil or granular materials.

The Mohr–Coulomb yield criterion may be expressed as:

$$\pm\frac{\sigma_1-\sigma_2}{2} = c-K\left(\frac{\sigma_1+\sigma_2}{2}\right)\ ;\ \pm\frac{\sigma_2-\sigma_3}{2} = c-K\left(\frac{\sigma_2+\sigma_3}{2}\right)\ ;\ \pm\frac{\sigma_3-\sigma_1}{2} = c-K\left(\frac{\sigma_3+\sigma_1}{2}\right)$$

where

$$m = \frac{\sigma_c}{\sigma_t}\ ,\quad K = \frac{m-1}{m+1}\ ;\quad c = \left(\frac{1}{m+1}\right)\sigma_c = \left(\frac{m}{m+1}\right)\sigma_t$$

and the parameters σ_c and σ_t are the yield (failure) stresses of the material in uniaxial compression and tension, respectively. If $K = 0$ then the Mohr–Coulomb criterion reduces to the Tresca–Guest criterion.

Figure 5 shows Mohr–Coulomb yield surface in the three-dimensional space of principal stresses. It is a conical prism and K determines the inclination angle of conical surface. Figure 6 shows Mohr–Coulomb yield surface in two-dimensional stress space. It is a cross section of this conical prism on the plane of σ_1,σ_2.

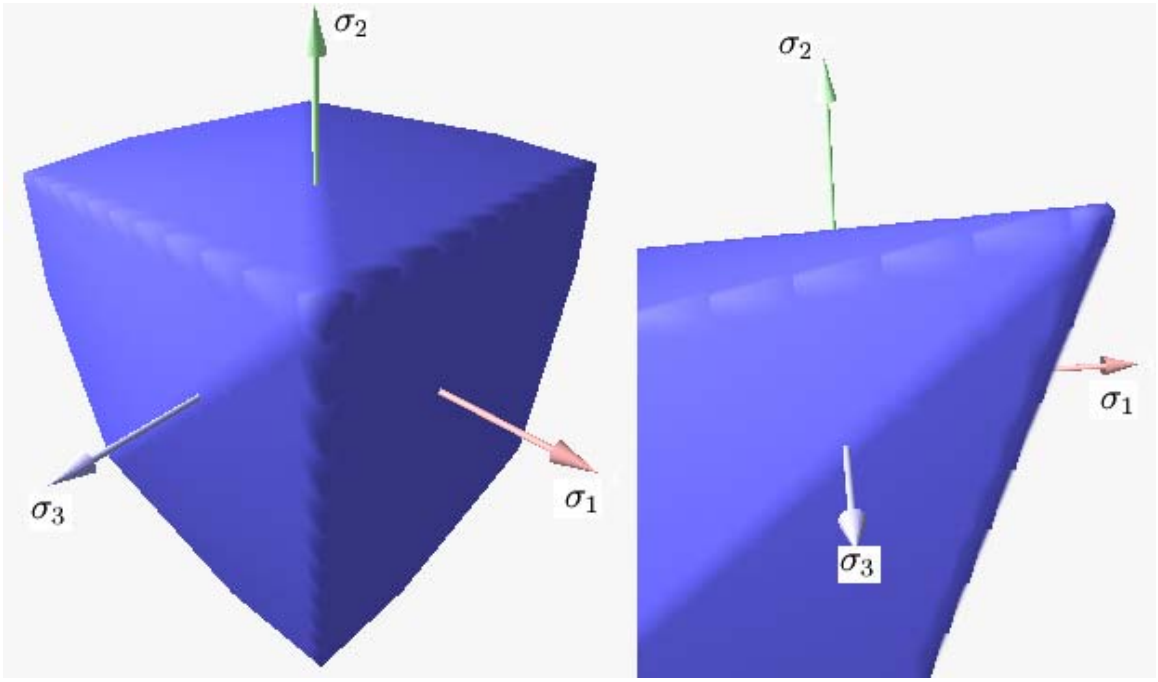

Figure 5: View of Mohr–Coulomb yield surface in 3D space of principal stresses

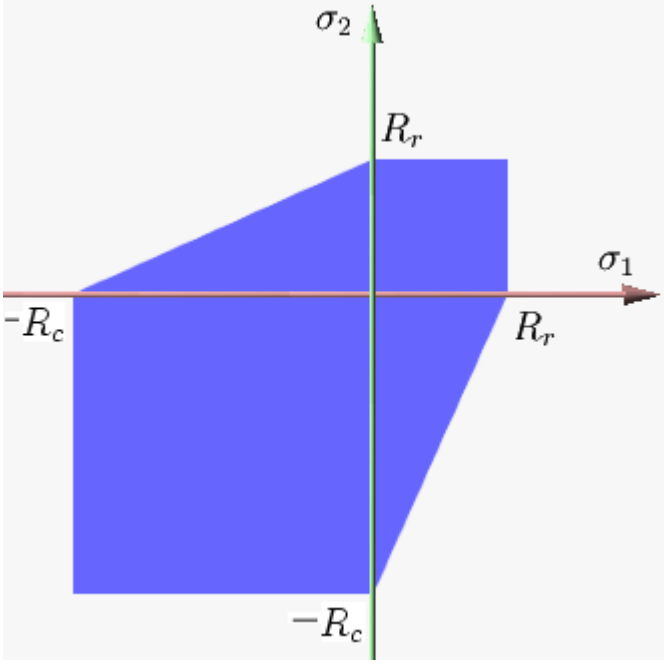

Figure 6: Mohr–Coulomb yield surface in 2D space (σ_1,σ_2)

The following formula was used to plot the surface in Fig. 5 :

$$\max\left(\frac{|\sigma_1-\sigma_2|}{2}-c+K\frac{\sigma_1+\sigma_2}{2},\ \frac{|\sigma_2-\sigma_3|}{2}-c+K\frac{\sigma_2+\sigma_3}{2},\ \frac{|\sigma_3-\sigma_1|}{2}-c+K\frac{\sigma_3+\sigma_1}{2}\right)=0$$

Drucker–Prager yield surface

The Drucker–Prager yield criterion has the function form

$$f(I_1, J_2) = 0\ .$$

This criterion is most often used for concrete where both normal and shear stresses can determine failure. The Drucker–Prager yield criterion may be expressed as

$$\alpha\left(\sigma_1+\sigma_2+\sigma_3\right)+\sqrt{\frac{(\sigma_1-\sigma_2)^2+(\sigma_2-\sigma_3)^2+(\sigma_3-\sigma_1)^2}{6}}=K$$

where

$$m=\frac{\sigma_c}{\sigma_t}\ ;\quad K=\frac{2\sigma_c}{\sqrt{3}(m+1)}\ ;\quad \alpha=\frac{m-1}{\sqrt{3}(m+1)}$$

and σ_c,σ_t are the uniaxial yield stresses in compression and tension respectively.

Figure 7 shows Drucker–Prager yield surface in the three-dimensional space of principal stresses. It is a regular cone. Figure 8 shows Drucker–Prager yield surface in two-dimensional space. The ellipsoidal-shaped elastic domain is a cross section of the cone on the plane of σ_1,σ_2; here it is shown enclosing the elastic domain for the Mohr–Coulomb yield criterion, although the converse scenario is also possible.

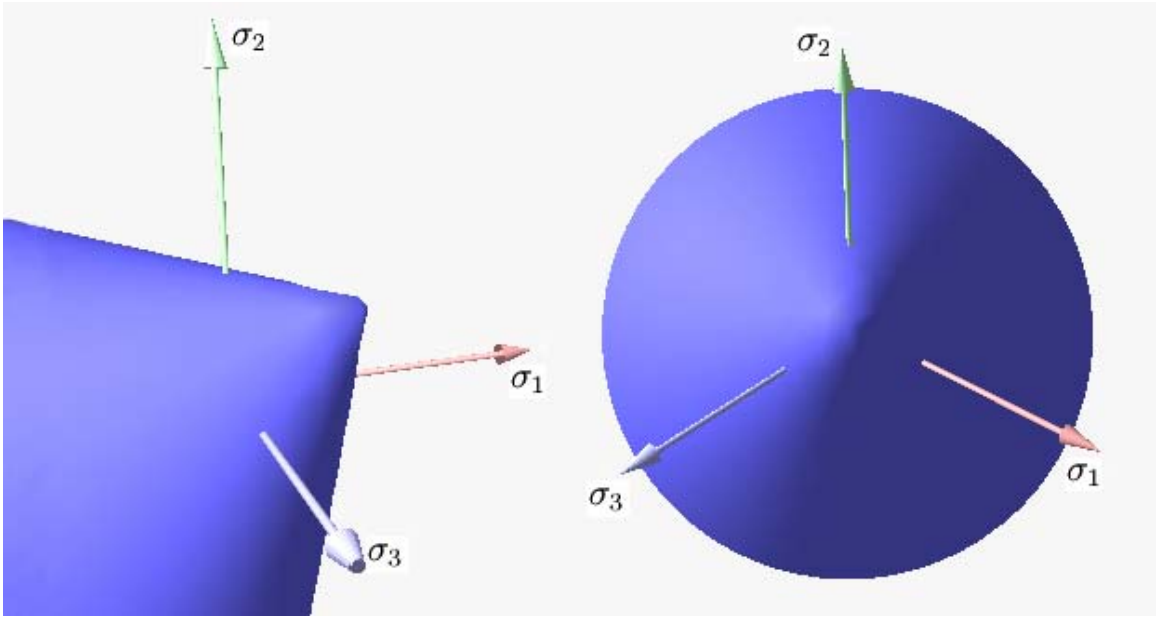

Figure 7: View of Drucker–Prager yield surface in 3D space of principal stresses

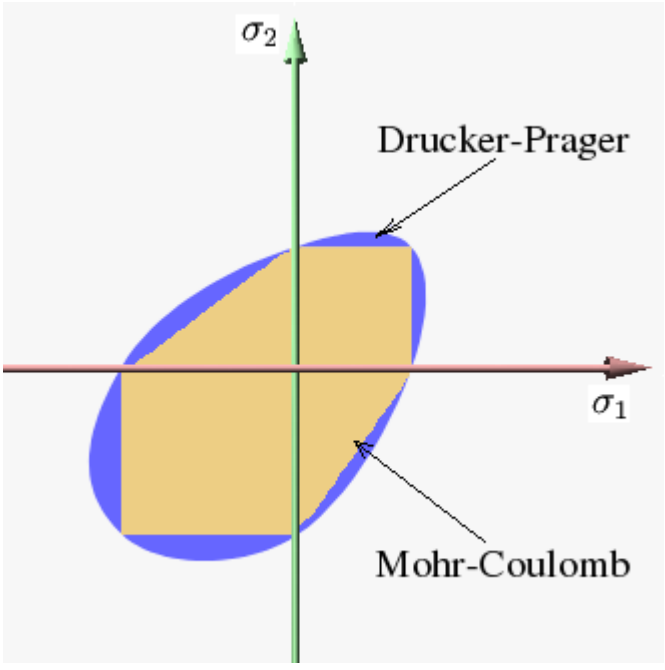

Figure 8: Drucker–Prager and Mohr–Coulomb yield surface in 2D space (σ_1,σ_2)

Bresler–Pister yield surface

The Bresler–Pister yield criterion is an extension of the Drucker–Prager yield criterion that uses three parameters.

The Bresler–Pister yield surface has the functional form

$$f(I_1, J_2) = 0 \ .$$

In terms of the principal stresses, this yield criterion may be expressed as

$$f := \frac{1}{\sqrt{6}}\left[(\sigma_1 - \sigma_2)^2 + (\sigma_2 - \sigma_3)^2 + (\sigma_3 - \sigma_1)^2\right]^{1/2} - c_0 - c_1\,(\sigma_1+\sigma_2+\sigma_3) - c_2\,(\sigma_1+\sigma_2+\sigma_3)^2$$

where c_0,c_1,c_2 are material constants. The additional parameter c_2 gives the yield surface a ellipsoidal cross section when viewed from a direction perpendicular to its axis. If σ_c is the yield stress in uniaxial compression, σ_t is the yield stress in uniaxial tension, and σ_b is the yield stress in biaxial compression, the parameters can be expressed as

$$c_1 = \left(\frac{\sigma_t - \sigma_c}{\sqrt{3}(\sigma_t + \sigma_c)}\right)\left(\frac{4\sigma_b^2 - \sigma_b(\sigma_c + \sigma_t) + \sigma_c\sigma_t}{4\sigma_b^2 + 2\sigma_b(\sigma_t - \sigma_c) - \sigma_c\sigma_t}\right)$$

$$c_2 = \left(\frac{1}{\sqrt{3}(\sigma_t + \sigma_c)}\right)\left(\frac{\sigma_b(3\sigma_t - \sigma_c) - 2\sigma_c\sigma_t}{4\sigma_b^2 + 2\sigma_b(\sigma_t - \sigma_c) - \sigma_c\sigma_t}\right)$$

$$c_0 = \frac{\sigma_c}{\sqrt{3}} + c_1\sigma_c - c_2\sigma_c^2$$

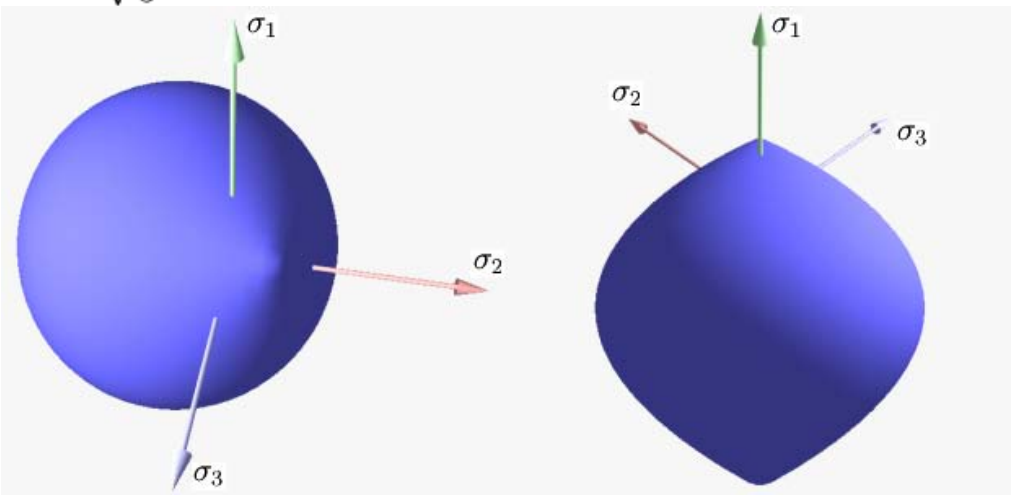

Figure 9: View of Bresler–Pister yield surface in 3D space of principal stresses

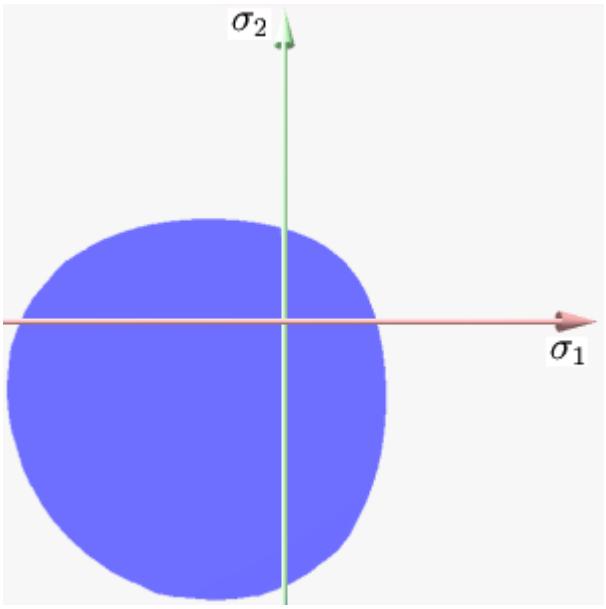

Figure 10: Bresler–Pister yield surface in 2D space (σ_1,σ_2)

Willam–Warnke yield surface

The Willam–Warnke yield criterion is a three-parameter smoothed version of the Mohr–Coulomb yield criterion that has similarities in form to the Drucker–Prager and Bresler–Pister yield criteria.

The yield criterion has the functional form

$$f(I_1, J_2, J_3) = 0 \ .$$

However, it is more commonly expressed in Haigh–Westergaard coordinates as

$$f(\xi, \rho, \theta) = 0 \ .$$

The cross-section of the surface when viewed along its axis is a smoothed triangle (unlike Mohr–Coulumb). The Willam–Warnke yield surface is convex and has unique and well defined first and second derivatives on every point of its surface. Therefore the Willam–Warnke model is computationally robust and has been used for a variety of cohesive-frictional materials.

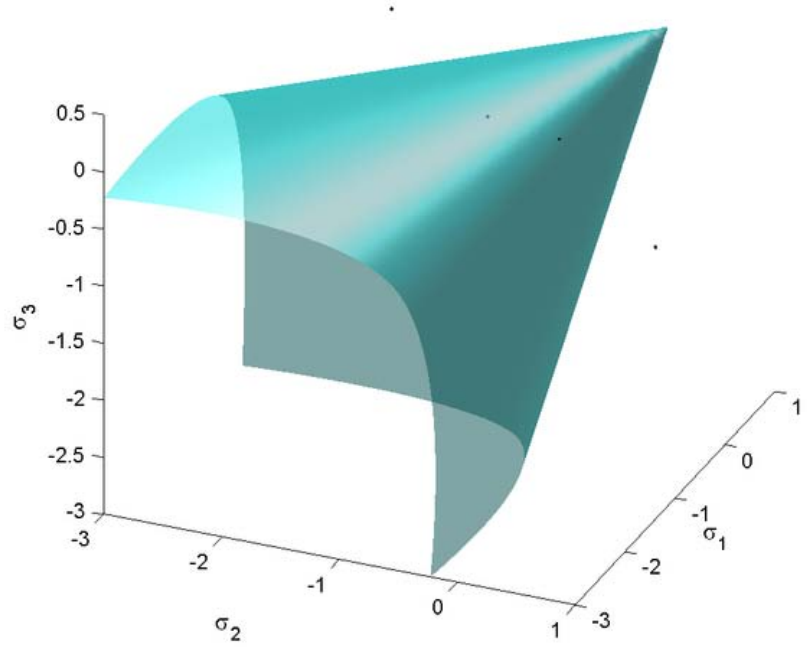

Figure 11: View of Willam–Warnke yield surface in 3D space of principal stresses

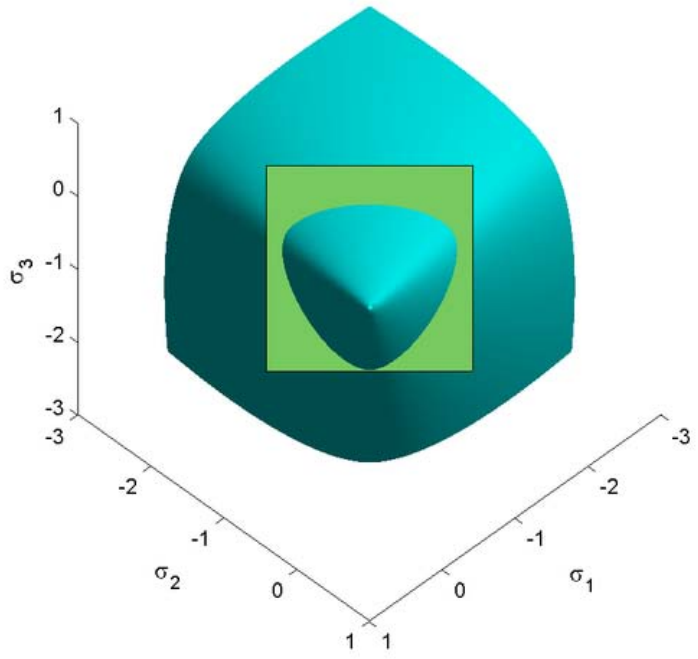

Figure 12: Willam–Warnke yield surface in the π-plane